PLOS PATHOGENS

Cyclooxygenase production of PGE$_2$ promotes phagocyte control of *A. fumigatus* hyphal growth in larval zebrafish

Savini Thrikawala[1], **Mengyao Niu**[2], **Nancy P. Keller**[2,3], **Emily E. Rosowski**[1]*

1 Department of Biological Sciences, Clemson University, Clemson, South Carolina, United States of America, **2** Department of Medical Microbiology and Immunology, University of Wisconsin-Madison, Madison, Wisconsin, United States of America, **3** Department of Bacteriology, University of Wisconsin-Madison, Madison, Wisconsin, United States of America

* erosows@clemson.edu

Abstract

Invasive aspergillosis is a common opportunistic infection, causing >50% mortality in infected immunocompromised patients. The specific molecular mechanisms of the innate immune system that prevent pathogenesis of invasive aspergillosis in immunocompetent individuals are not fully understood. Here, we used a zebrafish larva-*Aspergillus* infection model to identify cyclooxygenase (COX) enzyme signaling as one mechanism that promotes host survival. Larvae exposed to the pan-COX inhibitor indomethacin succumb to infection at a significantly higher rate than control larvae. COX signaling is both macrophage- and neutrophil-mediated. However, indomethacin treatment has no effect on phagocyte recruitment. Instead, COX signaling promotes phagocyte-mediated inhibition of germination and invasive hyphal growth. Increased germination and invasive hyphal growth is also observed in infected F0 crispant larvae with mutations in genes encoding for COX enzymes (*ptgs2a/b*). Protective COX-mediated signaling requires the receptor EP2 and exogenous prostaglandin E$_2$ (PGE$_2$) rescues indomethacin-induced decreased immune control of fungal growth. Collectively, we find that COX signaling activates the PGE$_2$-EP2 pathway to increase control *A. fumigatus* hyphal growth by phagocytes in zebrafish larvae.

Author summary

Invasive aspergillosis causes mortality in >50% of infected patients. It is caused by a free-living fungus *Aspergillus fumigatus* which releases thousands of airborne spores. While healthy individuals clear inhaled spores efficiently, in immunocompromised individuals these spores grow into filamentous hyphae and destroy lungs and other tissues causing invasive aspergillosis. The immune mechanisms that control this fungal growth in healthy people are still largely unknown. Here, we used a larval zebrafish model of *A. fumigatus* infection to determine that cyclooxygenase enzymes, which are the target of non-steroidal anti-inflammatory drugs such as aspirin and ibuprofen, are important to control the fungus. Innate immune cells use cyclooxygenase signaling to prevent hyphal growth and

tissue destruction. Our study provides new insights into the mechanisms that immune cells deploy to stop invasive growth of *A. fumigatus* and inform development of future strategies to combat invasive aspergillosis.

Introduction

Aspergillus fumigatus is a free-living saprophytic fungus which reproduces asexually by producing thousands of conidia or spores. Owing to their small size and hydrophobicity, spores become airborne causing widespread contamination both indoors and outdoors. It is estimated that an average person can inhale 100–1000 spores per day [1]. Although healthy immune systems can combat these spores, in immunocompromised individuals spores can germinate to form invasive hyphae which spread to multiple organs and tissues—a condition called invasive aspergillosis (IA) [1]. IA remains a major cause of mortality in immunocompromised patients, particularly individuals with hematological malignancies, bone marrow or solid-organ transplant recipients, HIV patients, ICU patients, and patients with altered lung conditions [2]. Despite the availability of anti-fungal drugs, the mortality rate of IA remains at ~50% [3–5]. Hence, it is imperative to develop novel strategies to target fungi and augment anti-fungal immune responses, but this requires a better understanding of immune cell-pathogen interactions. Innate immune cells act as the first line of defense against inhaled *A. fumigatus* conidia. However, the signaling and effector mechanisms that these cells use to inhibit fungal growth are not fully understood.

Eicosanoids, such as prostaglandins, are arachidonic acid-derived lipid signaling molecules that function in both an autocrine and paracrine manner by binding to their receptors and can have a variety of effects on immune cell function [6,7]. Prostaglandins are produced by prostaglandin endoperoxide synthases (PTGSs), also called cyclooxygenase (COX) enzymes. COX enzymes are the target of non-steroidal anti-inflammatory drugs such as aspirin, ibuprofen and indomethacin [8–10]. COX-derived prostaglandins can have either pro- or anti-inflammatory effects on innate immune cells, modulating both phagocyte recruitment and phagocyte functions [6,7,11]. In response to fungal pathogens, prostaglandin signaling is known to inhibit phagocytosis of *Candida albicans* by macrophages, H_2O_2-mediated fungicidal activity against *Paracoccidioides brasiliensis*, and M1 polarization of alveolar macrophages and killing of *Cryptococcus neoformans* [12–14]. However, the roles of COX activation and prostaglandins during *A. fumigatus* infections are not known.

Analyzing how given pathways affect specific aspects of dynamic host-pathogen interactions *in vivo* is challenging. The zebrafish larva-*Aspergillus* infection model overcomes many of these challenges, as larvae are transparent and allow for direct visualization of phagocyte-*Aspergillus* interactions through high-resolution repetitive imaging of the same larvae over the course of a multi-day infection [15]. Multiple steps in pathogenesis such as phagocyte recruitment, phagocytosis, spore killing, germination, and hyphal growth or clearance can be quantified using this live imaging technique [16]. Zebrafish have a well-conserved immune system with humans, but depend solely on their innate immune system for the first few weeks of their life, providing a window to study innate immune mechanisms with no interference from the adaptive system [17,18]. The zebrafish larva-*Aspergillus* model recapitulates multiple aspects of human IA: while immunocompetent larvae are resistant, immunocompromised larvae are susceptible to the infection and develop invasive hyphae [19,20].

Here we use this zebrafish larva-*Aspergillus* infection model to determine the role of the host COX pathway in phagocyte-mediated *A. fumigatus* clearance. We find inhibition of host

COX signaling increases spore germination and invasive growth of hyphae in infected larvae, thereby decreasing host survival. Genetic targeting of COX enzymes with CRISPR/Cas9 confirms that these host enzymes promote control of *A. fumigatus* germination and growth. COX signaling does not affect macrophage or neutrophil recruitment but instead activates these cells to target the fungus. Exogenous PGE_2 injection restores control of hyphae in COX-inhibited larvae, suggesting that PGE_2 is a major driver of COX-mediated control of fungal growth by phagocytes.

Results

Host cyclooxygenase inhibition decreases infected larval survival

Prostaglandins are lipid signaling molecules whose production is induced during inflammation via cyclooxygenase (COX) enzymes. We used the zebrafish larva-*Aspergillus* infection model to test the hypothesis that host COX signaling promotes larval survival and fungal clearance in an *A. fumigatus* infection. Wild-type *A. fumigatus* spores were microinjected into the hindbrain ventricle of 2 days post fertilization (dpf) larvae. Infected larvae were then exposed to the pan-COX inhibitor indomethacin or DMSO vehicle control immediately after injection and larval survival was monitored for 7 days. Indomethacin is a well-established non-steroidal anti-inflammatory drug that inhibits COX enzyme activation and prostaglandin synthesis [9,10] and is widely used in a variety of animal models including zebrafish [21,22]. Indomethacin-treated larvae succumb to infection at a significantly greater rate than control larvae (Fig 1A). Treatment with the COX1 inhibitor SC560 [23] or COX2 inhibitor meloxicam [21] also significantly increases infected larval mortality (S1A and S1B Fig). With each of these inhibitors, no significant decrease in survival was observed in PBS-injected mock-infected larvae (Figs 1A and S1A and S1B).

A. fumigatus also harbors three Ppo enzymes (PpoA, PpoB and PpoC) with high identity to vertebrate COX [24]. While a previous study reported that indomethacin does not affect the function of these enzymes [25], we wanted to confirm that the observed effects of indomethacin on infected larval survival are due to inhibition of host enzymes, not fungal enzymes. First, we confirmed that during the larval stage, zebrafish have detectable levels of COX activity (S1C Fig). Next, to determine the role of *A. fumigatus* Ppo enzymes, we infected zebrafish larvae with *A. fumigatus* spores lacking all three *ppo* genes (ΔppoA, ΔppoB, ΔppoC) (S2 Fig). Deletion
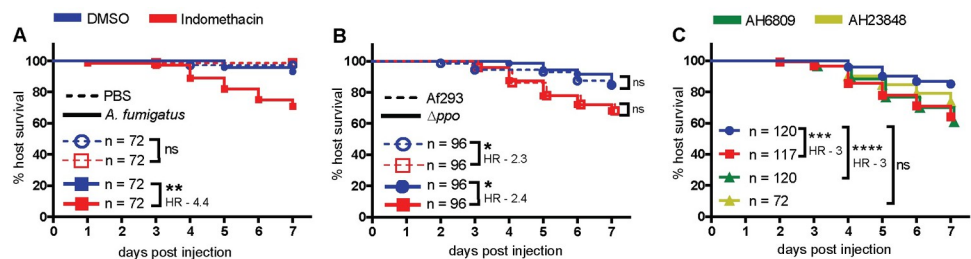
Fig 1. Host cyclooxygenase signaling promotes survival of *A. fumigatus*-infected larvae. (**A**) Survival of wild-type larvae injected at 2 dpf with TBK1.1 (Af293) *A. fumigatus* spores or PBS mock-infection in the presence of 10 μM indomethacin or DMSO vehicle control. (**B**) Survival of larvae injected at 2 dpf with *A. fumigatus* Af293 or Af293 triple-*ppo*-mutant (Δppo) spores and exposed to 10 μM indomethacin or DMSO vehicle control. (**C**) Survival of larvae injected at 2 dpf with TBK1.1 (Af293) spores and exposed to 10 μM indomethacin, 5 μM AH6809, 10 μM AH23848, or DMSO vehicle control. Data are pooled from at least three independent replicates, at least 24 larvae per condition, per replicate and the total larval N per condition is indicated in each figure. Cox proportional hazard regression analysis was used to calculate P values and hazard ratios (HR). Average injection CFUs: (A) 50, (B) Af293 = 40 and Δppo = 58, (C) 28.

https://doi.org/10.1371/journal.ppat.1010040.g001

of *ppo* enzymes had no effect on fungal virulence, as survival of larvae infected with triple-*ppo*-mutant *A. fumigatus* spores is similar to larvae infected with wild-type spores (Fig 1B). Additionally, indomethacin treatment decreased survival equally in larvae infected with triple-*ppo*-mutant and wild-type spores (Fig 1B). These data demonstrate that indomethacin inhibits host enzymes to compromise survival of *A. fumigatus*-infected larvae. Since no survival difference was observed in larvae infected with a triple-*ppo*-mutant, we focused on wild-type *A. fumigatus* for the remainder of the study.

Among COX-biosynthesized prostaglandins, prostaglandin E_2 (PGE_2) is a major product synthesized by phagocytes that moderates a range of inflammatory processes and has pro- or anti-inflammatory functions, depending on the receptor to which it binds [26]. PGE_2 elicits its actions via four different E type prostanoid receptors, EP1-4, with most immunomodulatory effects mediated via EP2 and EP4 [26]. Therefore, we tested if EP2 and 4 receptor antagonists affect the disease outcome of *A. fumigatus*-infected larvae. We used antagonists of EP2: AH6809 [27] and EP4: AH23848 [22,27,28] previously used in zebrafish larvae. Larvae exposed to AH6809 succumb to the infection at a similar rate as indomethacin-exposed larvae, both with a hazard ratio of 3 compared to control larvae, while AH23848-exposed larvae show no significant difference in survival compared to control (Fig 1C). These data suggest that COX signaling promotes *A. fumigatus*-infected larval survival via a PGE_2-EP2 signaling pathway.

Both macrophages and neutrophils use cyclooxygenase signaling to combat *A. fumigatus* infection

We next sought to determine which innate immune cells utilize COX signaling to fight *A. fumigatus* infection. Macrophages and neutrophils are the primary immune cells that combat *A. fumigatus* infection in zebrafish larvae [20]. To determine if these cell types play a role in COX-mediated host responses, we inhibited development of both phagocytes by knocking down *pu.1 (spi1b)* via morpholino injection [29]. If COX signaling activates phagocytes to clear the infection, we expect that indomethacin treatment of larvae that are already depleted of phagocytes would have no effect on larval survival. Larvae were injected with *A. fumigatus* spores or PBS and exposed to indomethacin or DMSO. Indomethacin exposure significantly decreases survival of larvae injected with a control morpholino but has no effect on *pu.1* morphants (Figs 2A and S3A), suggesting that COX-mediated host protection is phagocyte-dependent.

Then we interfered with macrophage and neutrophil function individually to determine if each cell type is required for COX-mediated host protection. We injected 1 dpf larvae with clodronate liposomes to deplete macrophages or PBS liposomes as a control. As observed previously, macrophage-depleted larvae rapidly succumb to the infection (Fig 2B) [20]. However, indomethacin exposure further decreases the survival of macrophage-depleted larvae (Fig 2B). While indomethacin treatment makes control larvae 8.4 times more likely to succumb to infection, clodronate liposome-injected larvae are only 1.7 times more likely to succumb upon indomethacin treatment (Fig 2B), suggesting that macrophages partially mediate the host-protective effects of COX signaling, but that even in the absence of macrophages COX signaling increases host survival. Larvae injected with clodronate liposomes and then given a PBS mock-infection also have lower survival upon indomethacin treatment, suggesting that some of this death may be due to the effects of the clodronate alone, although this difference in PBS mock-infected larvae is not statistically significant (S3B Fig).

We next tested the survival of neutrophil-defective (*mpx:rac2D57N*) infected larvae. In these larvae neutrophils are unable to migrate to the infection site [30]. As found previously, neutrophil-defective larvae are more susceptible to *A. fumigatus* infection than wild-type
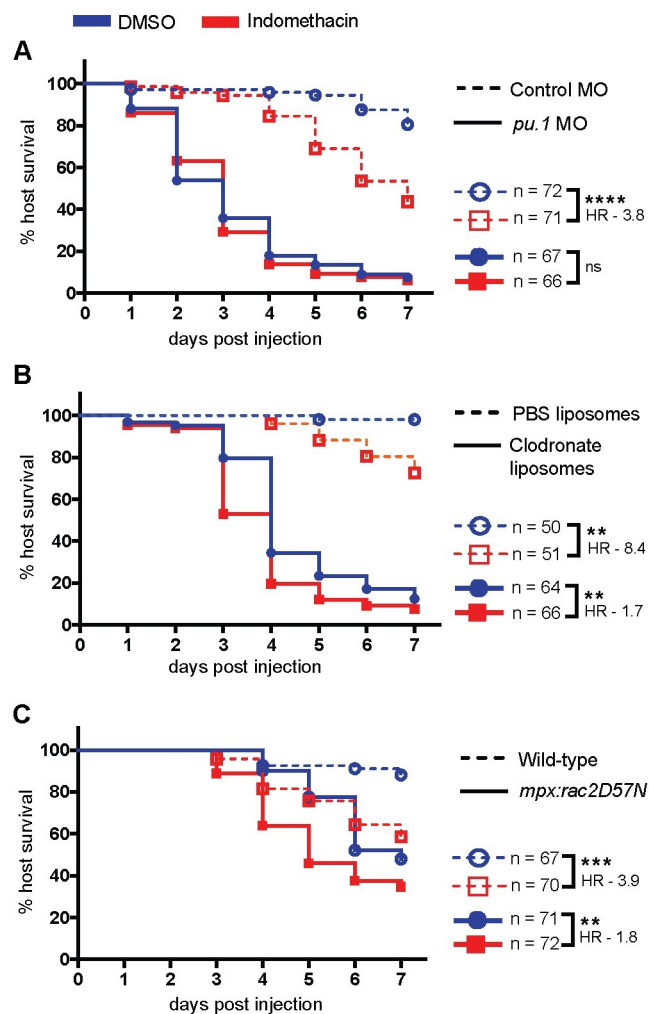
Fig 2. Cyclooxygenase-mediated host protection depends on phagocytes. Survival of larvae injected with TBK1.1 (Af293) spores at 2 dpf. **(A)** Development of phagocytes was inhibited by *pu.1* morpholino (MO). Control larvae received standard control MO. **(B)** Macrophages were depleted via clodronate liposome i.v. injection at 1 dpf. Control larvae received PBS liposomes. **(C)** Neutrophil-defective larvae (*mpx:rac2D57N*) were compared to wild-type larvae. Data are pooled from three independent replicates, at least 10 larvae per condition, per replicate and the total larval N per condition is indicated in each figure. Cox proportional hazard regression analysis was used to calculate P values and hazard ratios (HR). Average injection CFUs: (A) control MO = 25, *pu.1* MO = 24, (B) PBS liposomes = 20, clodronate liposomes = 23, (C) wild-type = 26, *mpx:rac2D57N* = 22.

controls (Fig 2C) [20,31]. Indomethacin exposure further decreases survival of neutrophil-defective larvae (Fig 2C). Compared to wild-type larvae which are 3.9 times more likely to succumb to infection, neutrophil-defective larvae are only 1.8 times more likely to succumb to infection, suggesting that neutrophils also partially mediate the host-protective effects of COX signaling, but that other cell types can be involved. Lack of neutrophils has no effect on survival of mock-infected larvae treated with indomethacin (S3C Fig). Together, these data demonstrate that both macrophages and neutrophils participate in COX-mediated responses to promote survival of *A. fumigatus*-infected zebrafish larvae.

To further ascertain the roles of each cell type in COX signaling, we determined whether macrophages and neutrophils sorted from 3 dpf larvae express genes in the COX/PGE$_2$

pathway. Zebrafish possess two copies of COX2: *prostaglandin-endoperoxide synthase-2a* and *-2b* (*ptgs2a* and *ptgs2b*) [32], both of which we find expressed in macrophages and neutrophils, while neither cell type expresses the zebrafish COX1 gene (*ptgs1*) (S4 Fig). COX enzymes synthesize PGH_2, an intermediate that is converted to PGE_2 by prostaglandin E synthases, which are either membrane-bound (mPges) or cytosolic (cPges) [6]. All zebrafish *pges* genes are expressed by macrophages, while neutrophils express only the cytosolic versions (S4 Fig). At least one EP2 receptor gene (*ep2a* or *ep2b*) is expressed in both phagocytes (S4 Fig). These data demonstrate that both macrophages and neutrophils express the machinery needed to generate and respond to COX/PGE_2 signaling.

Cyclooxygenase activity is not required for phagocyte recruitment

We next sought to define how the innate immune response is altered by COX inhibition. COX-synthesized prostaglandins are chemical messengers that can function to recruit immune cells to infection sites, and we wondered whether COX inhibition affects macrophage or neutrophil recruitment to *A. fumigatus* infection [7,20]. Zebrafish larvae expressing GFP in macrophages (*Tg(mpeg1:H2B-GFP)*) or BFP in neutrophils (*Tg(lyz:BFP)*) were infected with *A. fumigatus* spores expressing mCherry, and treated with indomethacin or DMSO vehicle control and we enumerated the number of macrophages and neutrophils at the infection site through daily confocal imaging (Fig 3A).

As described previously, macrophages are recruited starting at 1 day post infection (dpi) and form clusters around spores starting at 2–3 dpi (Fig 3B), with neutrophils primarily responding after spores germinate (Fig 3C) [20]. The number of recruited macrophages (Fig 3D), macrophage cluster area (Fig 3E), and the number of recruited neutrophils (Fig 3F) are not significantly different between indomethacin- and DMSO-exposed groups at days 1, 2, and 3 post infection. At 5 dpi, however, more macrophages (Fig 3D) and neutrophils (Fig 3F) are found at the infection site in indomethacin-treated larvae. Fungal germination occurs at these later time stages and attracts more immune cells. To control for this variable, we analyzed the number of macrophages and neutrophils in each larva relative to the day germination and invasive hyphae were first observed. Using this normalization, we find that macrophage numbers (Fig 3G) and neutrophil numbers (Fig 3H) are similar between the two conditions at each stage of fungal pathogenesis. Overall, our results indicate that phagocyte recruitment is not dependent on COX activation.

Cyclooxygenase activity does not promote spore killing

We next hypothesized that the functions of these phagocytes are modulated by COX signaling. The initial response of macrophages is to phagocytose injected spores and activate spore killing mechanisms [19,20]. To determine if COX inhibition affects spore killing, we used a live-dead staining method in which *A. fumigatus* spores expressing YFP are coated with AlexaFluor546 and injected into zebrafish larvae expressing mTurquoise in macrophages [20,33]. Larvae were imaged with confocal microscopy at 2 dpi, and we enumerated the number of live versus dead spores. Live spores are visualized as YFP signal surrounded by AlexaFluor signal, while dead spores only have AlexaFluor signal (Fig 4A). The percentage of live spores is similar in indomethacin and DMSO groups both within macrophages and in the whole imaged hindbrain area (Fig 4B). To confirm these results, we also measured the overall fungal burden in indomethacin- or DMSO-treated larvae over the 7-day infection period with CFU counts. Consistent with live-dead staining, the fungal burden is similar between DMSO- and indomethacin-exposed larvae throughout the infection (Figs 4C and S5), indicating that COX signaling does not drive spore clearance.
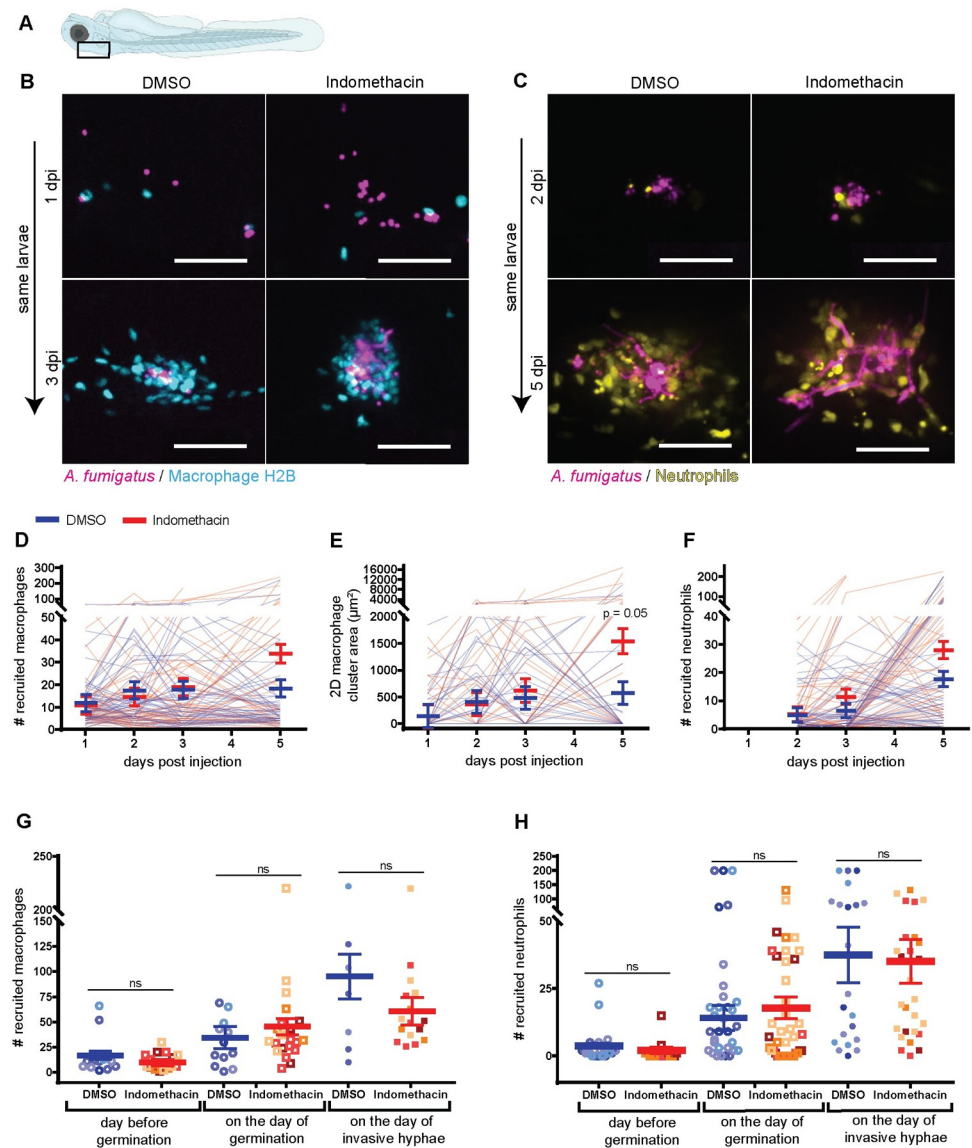
Fig 3. Cyclooxygenase inhibition does not alter phagocyte recruitment. Larvae were injected with mCherry-expressing *A. fumigatus* TBK5.1 (Af293) spores at 2 dpf. After injection larvae were exposed to 10 μM indomethacin or DMSO vehicle control and were imaged through 5 dpi. **(A)** Schematic showing the infection and imaging area of zebrafish larvae (created with BioRender.com). **(B, D, E, G)** Macrophage nuclear-labeled *Tg(mpeg1:H2B-GFP)* larvae were imaged at 1, 2, 3, and 5 dpi. **(C, F, H)** Neutrophil-labeled *Tg(lyz:BFP)* larvae were imaged at 2, 3, and 5 dpi. (B, C) Representative z-projection images showing macrophage and neutrophil recruitment. Scale bars = 50 μm. (D) Number of macrophages recruited, (E) 2D macrophage cluster area, and (F) number of neutrophils recruited were quantified. Each line represents an individual larva followed for the entire course of infection and bars represent pooled emmeans ± SEM from four independent replicates, at least 12 larvae per condition, per replicate. P values were calculated by ANOVA. (G) Number of macrophages and (H) neutrophils one day before germination occurred, on the day of germination, and on the day invasive hyphae occurred were quantified. Bars represent pooled emmeans ± SEM from all larvae with germination from four independent replicates. Data points represent individual larva and are color coded by replicate. P values were calculated by ANOVA.

https://doi.org/10.1371/journal.ppat.1010040.g003

Cyclooxygenase inhibition decreases immune control of fungal germination

As spore killing is not affected by COX inhibition, we next hypothesized that immune control of the next stages in fungal pathogenesis—spore germination and invasive hyphal growth—is
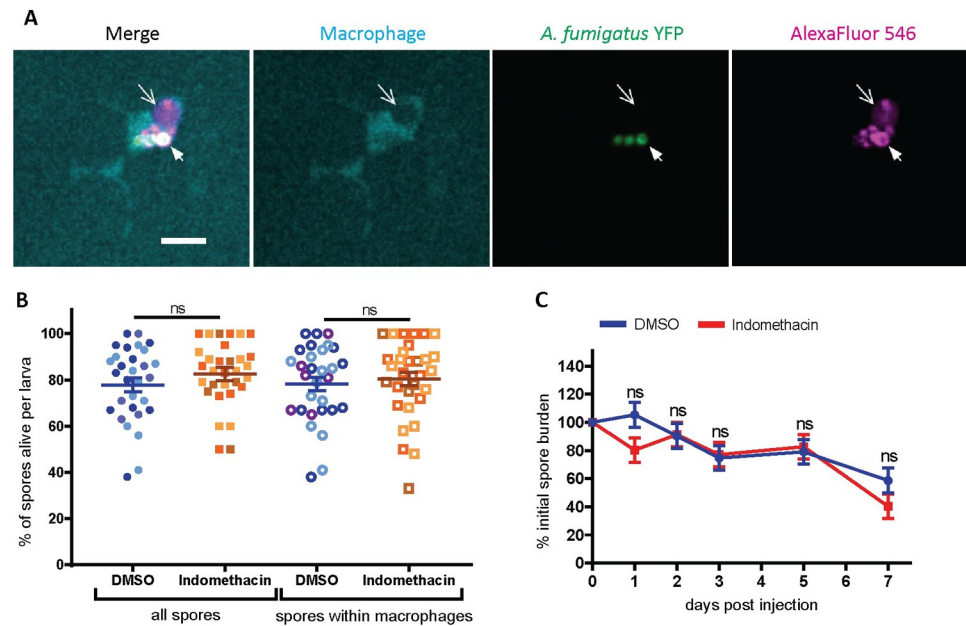
Fig 4. Cyclooxygenase inhibition does not affect spore killing. (A, B) Macrophage-labeled larvae *Tg(mfap4: mTurquoise2)* were injected with YFP-expressing *A. fumigatus* TBK1.1 (Af293) spores coated with AlexaFluor 546 at 2 dpf, exposed to 10 µM indomethacin or DMSO vehicle control, and imaged at 2 dpi. (A) Representative images showing live (white arrow) and dead (open arrow) spores within a macrophage. Scale bar = 10 µm. (B) The percentage of live spores in the hindbrain, and specifically within macrophages, per larvae. Each data point represents an individual larvae, color-coded by replicate (indomethacin n = 31, DMSO n = 30). Bars represent pooled emmeans ± SEM from three independent replicates, P values calculated by ANOVA. **(C)** Wild-type larvae were injected with TBK1.1 (Af293) spores at 2 dpf, exposed to 10 µM indomethacin or DMSO vehicle control, and fungal burden was quantified by homogenizing and plating individual larvae for CFUs at multiple days post injection. Eight larvae per condition, per dpi, per replicate were quantified, and the number of CFUs at each dpi is represented as a percentage of the initial spore burden. Bars represent pooled emmeans ± SEM from three individual replicates, P values calculated by ANOVA. Average injection CFUs: 27. Non-normalized raw CFU data is presented in S5 Fig.

https://doi.org/10.1371/journal.ppat.1010040.g004

modulated by COX signaling. To monitor spore germination and hyphal growth in larvae, we infected larvae with *A. fumigatus* spores expressing mCherry and imaged at 1, 2, 3 and 5 dpi with confocal microscopy. We find spore germination in both indomethacin- and DMSO-exposed larvae (Fig 5A). However, both the rate at which larvae are observed to have germination inside of them and the total percentage of larvae that harbor germinated spores is significantly higher in the presence of indomethacin (Fig 5B).

Since germination is increased upon indomethacin treatment, we wanted to confirm again that the effects of indomethacin are on the host and that indomethacin does not directly alter *A. fumigatus* germination. To test this, *A. fumigatus* spores were inoculated *in vitro* in liquid RPMI medium in the presence of indomethacin or DMSO and the percentage of germinated spores was scored at 2-hour intervals. We find no difference in the rate of germination between indomethacin- and DMSO-treated spores (S6 Fig). Therefore, our data demonstrate that indomethacin decreases host immune cell-mediated control of *A. fumigatus* germination.

Cyclooxygenase inhibition decreases immune control of invasive hyphal growth

After germination, *A. fumigatus* hyphae branch and grow into a network disrupting the host tissue. The cumulative percentage of larvae with invasive hyphae (as defined by branched
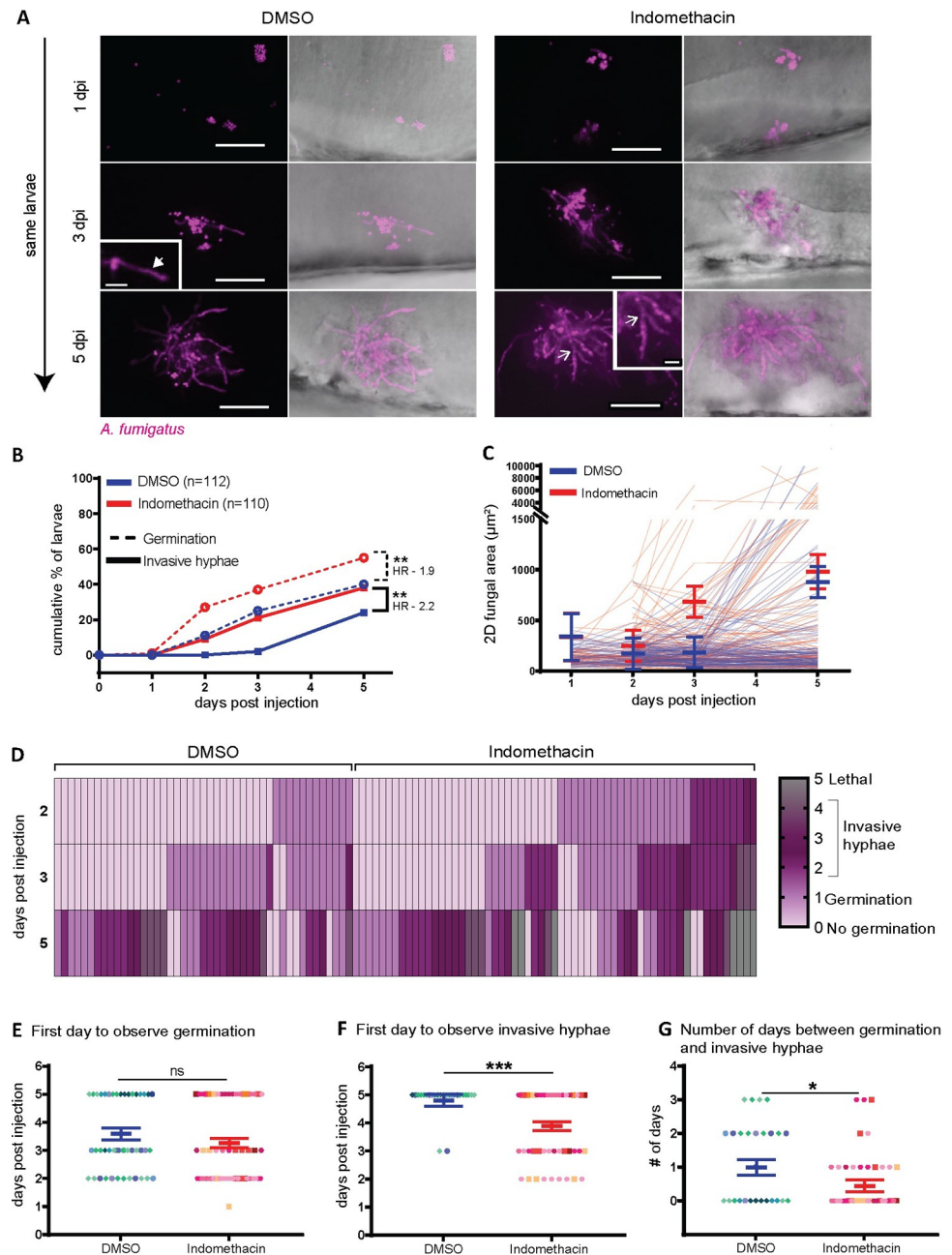
Fig 5. Cyclooxygenase inhibition decreases immune control of fungal germination and invasive hyphal growth.
Zebrafish larvae were injected with mCherry-expressing TBK5.1 (Af293) spores at 2 dpf, exposed to 10 μM indomethacin or DMSO vehicle control and imaged at 1, 2, 3, and 5 dpi. **(A)** Representative images showing spore germination (inset white arrow) and invasive hyphae (branched hyphae, inset open white arrow). Scale bar = 50 μm (10 μm in insets). **(B)** Cumulative percentage of larvae with germination (dotted line) and invasive hyphae (solid line) through 5 dpi. Cox proportional hazard regression analysis was used to calculate P values and hazard ratios (HR). **(C)** 2D fungal area was quantified from image z projections. Each line represents an individual larva and bars represent pooled emmeans ± SEM from 8 independent replicates, at least 12 larvae per condition, per replicate. **(D)** Severity of fungal growth was scored for all larvae and displayed as a heatmap. Representative images for each score can be found in S7 Fig. **(E-G)** In larvae in which (E) germination (indomethacin n = 61, DMSO n = 45) and (F) invasive hyphae occurred (indomethacin n = 42, DMSO n = 27), the day on which each was first observed is plotted. (G) The number of days between germination and invasive hyphae was also calculated. Bars represent pooled emmeans ± SEM from eight individual replicates, P values calculated by ANOVA. Each data point represents an individual larvae, color-coded by replicate.

https://doi.org/10.1371/journal.ppat.1010040.g005

hyphal growth (S7 Fig)) is also significantly higher with indomethacin treatment (Fig 5B). We also quantified the hyphal burden by measuring the fungal area, finding more extensive hyphal growth in indomethacin-treated larvae at both 3 and 5 dpi, although this difference is not statistically significantly (Fig 5C), likely due to high variability between larvae and the large number of indomethacin-treated larvae that succumbed to infection before 5 dpi (Fig 1A).

Next, we rated the severity of fungal growth on a scale of 0 to 4, from no germination to severe invasive growth of hyphae, and a lethal score of 5 (S7 Fig), focusing only on larvae that had germination within them at some point in the experiment. Severe growth of invasive hyphae is prominent in larvae exposed to indomethacin, eventually causing mortality (Fig 5D). Although germination occurred in the vehicle control group, these larvae are able to delay invasive growth compared to indomethacin-treated larvae (Fig 5D), suggesting that the major defect in these larvae is a failure to control hyphal growth post-germination. To quantify this time of delay between appearance of germination and invasive hyphae, we analyzed the timeline of first appearance of germlings and invasive hyphae in larvae more closely. We quantified the day germination was first observed, the day invasive hyphae was first observed, and the time between these two occurrences. The day to first observe germination was similar between the two groups (Fig 5E). However, invasive hyphae appear significantly earlier after both initial infection (Fig 5F) and after germination (Fig 5G) in indomethacin-exposed larvae. Once spores are germinated, invasive hyphae appear on average ~1 day later in control larvae, while in indomethacin-treated larvae, this growth only takes an average of ~0.5 days (Fig 5G). We also used microscopy to determine fungal growth in larvae exposed to the EP2 antagonist AH6809. Blockage of this receptor also leads to increased spore germination and invasive hyphal growth at 3 dpi at a level similar to indomethacin (S8 Fig). Together, these results suggest that COX-PGE$_2$ signaling promotes phagocyte-mediated control of invasive hyphal growth.

Neutrophils are thought to be the major phagocyte that targets and kills invasive hyphae. In *irf8*^{-/-} larvae which lack macrophages and have an abundance of neutrophils, neutrophils destroy fast-germinating strains of *A. fumigatus* such as CEA10 within a few days [20]. We therefore decided to use this infection scenario to specifically test the requirement for COX signaling in neutrophil-mediated hyphal killing. We infected *irf8*^{-/-} larvae with CEA10 spores and isolated larvae for CFU enumeration at 0, 1, and 2 dpi. CFUs from *irf8*^{-/-} were normalized to CFUs of *irf8*^{+/+}/*irf8*^{+/-} at each dpi for each condition. At 2 dpi in DMSO-treated larvae, ~26% of the fungal burden remains in *irf8*^{-/-} larvae compared to macrophage-sufficient larvae (*irf8*^{+/+} or *irf8*^{+/-}), demonstrating the neutrophil-mediated clearance of fungus that occurs in these larvae (S9A Fig). Fungal clearance is slightly alleviated but not significantly different in indomethacin-exposed *irf8*^{-/-} larvae, suggesting that COX signaling may promote but is not required for neutrophil-mediated killing of hyphae (S9A Fig). Similar to infection with Af293-derived strains, CEA10-infected larvae also succumb to the infection at a higher rate in the presence of indomethacin both in *irf8*^{+/+}/*irf8*^{+/-} and *irf8*^{-/-} backgrounds (S9B Fig).

CRISPR-Cas9 targeting of COX enzyme genes also results in decreased control of spore germination and invasive fungal growth

One explanation for the observed effects of indomethacin specifically on control of later stages in fungal pathogenesis is a delay in drug absorption and accumulation at the infection site. To test this, we tried pre-treating larvae and treating larvae with a higher indomethacin concentration, but both conditions caused toxicity as evidenced by high mortality in mock-infected larvae (S10 Fig). To avoid these issues of drug absorption and to confirm the role of host COX
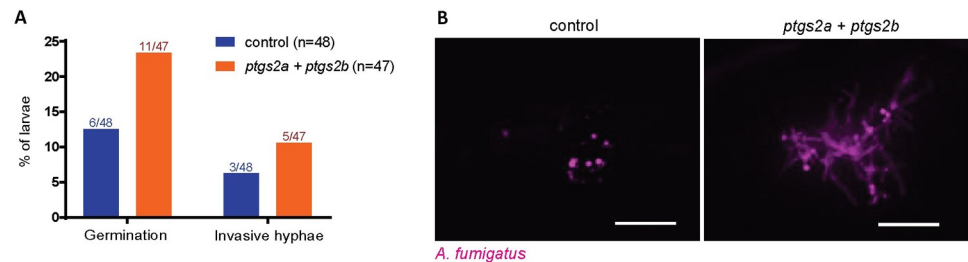
Fig 6. Loss of functional *ptgs* genes decreases immune control of fungal germination and invasive hyphae.
Embryos were injected with gRNAs targeting *ptgs2a* and *ptgs2b* or control gRNAs for *gfp* and Cas9 protein. F0 crispant larvae were then injected with GFP-expressing TBK1.1 (Af293) spores at 2 dpf and imaged at 3 dpi. **(A)** Percentage of larvae with germination or invasive hyphae. Data are pooled from two independent replicates, at least 23 larvae per condition, per replicate. Average injection CFUs: control = 38, *ptgs2a/2b* = 39. **(B)** Representative images showing hyphal growth in each condition. Scale bar = 50 μm.

https://doi.org/10.1371/journal.ppat.1010040.g006

enzymes in controlling *A. fumigatus* spore germination and invasive fungal growth, we used CRISPR/Cas9 to target both zebrafish COX2 genes: *ptgs2a* and *ptgs2b*. F0 larvae injected with gRNAs targeting both genes or control gRNAs were infected with *A. fumigatus* spores expressing GFP and imaged at 3 dpi. PCR of genomic DNA flanking the gRNA target sites confirmed efficient DNA alteration (S11 Fig). In *ptgs*-targeted larvae, we observed an increased occurrence of both spore germination and invasive hyphal growth (Fig 6), confirming that host COX enzymes increase the ability of immune cells to control these later stages of fungal pathogenesis.

Exogenous PGE$_2$ rescues immune control of hyphal growth in the presence of indomethacin

So far we have established that COX signaling promotes macrophage- and neutrophil-mediated control of germination and invasive hyphal growth in an *A. fumigatus* infection. It is likely that COX signaling acts via a PGE$_2$-EP2 signaling axis, as EP2 receptor antagonist-treated infected larvae have increased fungal growth (S8 Fig) and succumb to infection at the same rate as indomethacin-treated larvae (Fig 1C). We therefore tested if exogenous PGE$_2$ can rescue the effects of indomethacin treatment in infected larvae. Since PGE$_2$ is short-lived and elicits short-range effects, we injected *A. fumigatus*-infected, indomethacin- or DMSO-treated larvae with PGE$_2$ or DMSO vehicle control into the hindbrain at 1 dpi. PGE$_2$ injection partially rescues survival of indomethacin-treated larvae, although the effect is not statistically significant (Fig 7A). To determine if PGE$_2$ can rescue indomethacin-inhibited functions of phagocytes against invasive fungal growth, we imaged the larvae at 3 dpi. As seen previously, indomethacin treatment increases the percentage of larvae harboring both germination and invasive hyphae at 3 dpi (Fig 7B). PGE$_2$ supplementation rescues these phenotypes, decreasing germination and development of invasive hyphae (Fig 7B and 7C), without affecting phagocyte recruitment (S12A and S12B Fig). However, PGE$_2$ injection cannot increase the survival of either wild-type or neutrophil-defective larvae not treated with indomethacin (Figs 7A and S12C).

In these experiments, in the absence of indomethacin treatment, we found increased fungal germination and invasive hyphae upon PGE$_2$ injection, although these differences were not statistically significant (Fig 7B). To test if PGE$_2$ can directly act on spores to promote germination, we quantified *A. fumigatus* germination *in vitro* in the presence of exogenous PGE$_2$, but did not find any effect (Fig 7D). PGE$_2$ levels must be precisely controlled and balanced and an alternative explanation is that high levels of PGE$_2$ without concomitant indomethacin-
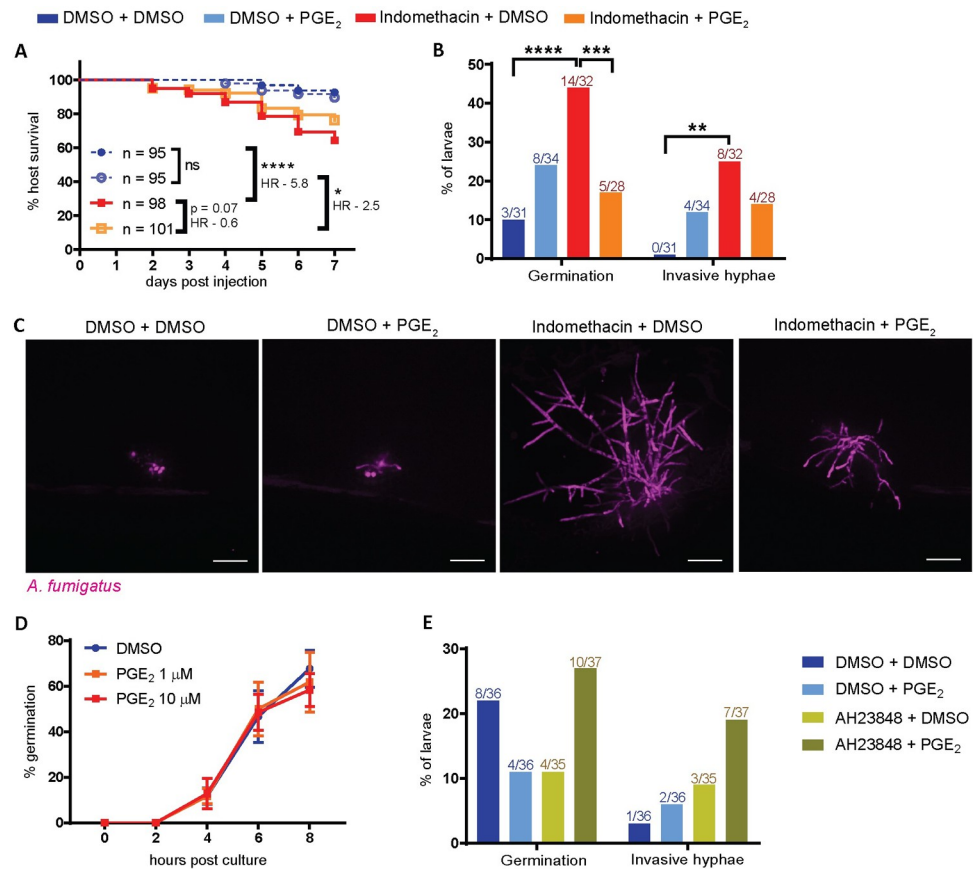
Fig 7. Exogenous PGE$_2$ can rescue the indomethacin-mediated increase in fungal germination and hyphal growth.
Larvae were injected with mCherry-expressing TBK5.1 (Af293) spores and exposed to 10 μM indomethacin or DMSO
vehicle control at 2 dpf. At 1 dpi, larvae were injected with 10 μM PGE$_2$ or DMSO vehicle control. **(A)** Survival of wild-
type larvae was monitored. Cox proportional hazard regression analysis was used to calculate P values and hazard
ratios (HR). Data are pooled from four independent replicates, at least 23 larvae per condition, per replicate and total
larval N per condition is indicated. Average injection CFUs: 40. **(B-C)** Larvae were imaged at 3 dpi. (B) Percentage of
larvae with germination and invasive hyphae. Data are pooled from three independent replicates, at least 8 larvae per
condition, per replicate, P values calculated by Fisher's Exact Test. (C) Representative images showing hyphal growth
in each condition. Scale bars = 50 μm. **(D)** TBK1.1 (Af293) spores were inoculated into RPMI media in the presence of
1 μM PGE$_2$, 10 μM PGE$_2$, or DMSO vehicle control. Every 2 hours, an aliquot of spores was removed and scored for
germination. Points represent pooled means ± SEM from two independent replicates. **(E)** Larvae were injected with
GFP-expressing TBK1.1 (Af293) spores and exposed to 5 μM AH23848 or DMSO vehicle control at 2 dpf. At 1 dpi,
larvae were injected with 10 μM PGE$_2$ or DMSO vehicle control. Larvae were imaged at 3 dpi and the percentage of
larvae with germination and invasive hyphae in each condition was calculated. Data are pooled from three
independent replicates, at least 11 larvae per condition, per replicate, P values calculated by Fisher's Exact Test.

mediated COX inhibition promote an anti-inflammatory environment via the EP4 receptor,
leading to lowered immune control of fungal growth [28]. Therefore, we tested if excess PGE$_2$
still leads to increased fungal germination and invasive hyphal growth when the EP4 receptor
is also blocked. Infected larvae exposed to the EP4 antagonist AH23848 were injected with
PGE$_2$ at 1 dpi. However, in these experiments, PGE$_2$ injection alone did not cause increased
fungal growth, possibly due to small differences in injection volume, further underlining how
small differences in PGE$_2$ levels can lead to different outcomes. Interestingly, however, expo-
sure to AH23848 alone or in combination with PGE$_2$ increased invasive hyphal growth in
infected larvae, although these differences were not statistically significant (Fig 7E). These data
together with the slightly increased mortality of infected larvae in the presence of AH23848
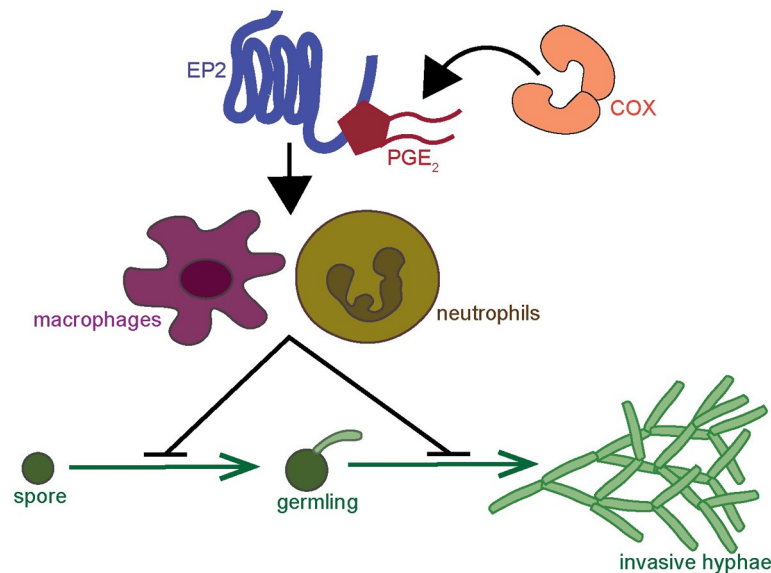
Fig 8. Model of cyclooxygenase signaling in response to *A. fumigatus* growth. COX enzymes produce prostaglandin signaling molecules, including PGE_2. PGE_2 can bind to the EP2 receptor to exert pro-inflammatory effects. In zebrafish larvae injected with *A. fumigatus*, this signaling activates both macrophages and neutrophils to inhibit spore germination and development of invasive hyphal growth.

https://doi.org/10.1371/journal.ppat.1010040.g008

(Fig 1D) suggest that EP4 may also play a minor role in mediating immune cell-mediated fungal growth control. Collectively, our findings demonstrate that COX-mediated PGE_2 production and signaling via the EP2 receptor promotes phagocyte-mediated control of *A. fumigatus* germination and hyphal growth (Fig 8).

Discussion

Healthy immune systems can contain and kill *A. fumigatus* spores despite the fact that hundreds of spores can be inhaled per day. While the physiological role of macrophages and neutrophils in this context is well-appreciated, the molecular mechanisms that each of these cell types use to combat each stage of fungal pathogenesis are not fully understood. The critical step in *A. fumigatus* pathogenesis is the transition from dormant spore to hyphal growth, causing tissue destruction. Here, we used a zebrafish larva-*A. fumigatus* infection model to identify COX-PGE_2 signaling as one mechanism that promotes control of this transition to invasive hyphae by both macrophages and neutrophils (Fig 8).

To investigate the role of COX signaling in phagocyte responses we used indomethacin, a pan-COX inhibitor, as well as COX1- and COX2-specific inhibitors. We find that activity of both enzymes promotes survival of *A. fumigatus*-infected larvae. Broadly, COX1 activity is involved in tissue homeostasis while COX2 is inducible and is involved in responses to inflammatory stimuli [6]. However, evidence suggests that both isoforms are activated during inflammation. Mice lacking COX1 have impaired inflammatory responses [34], and COX1 is activated in response to LPS-induced inflammation in humans [35]. Zebrafish have one functional isoform of COX1 and two functional orthologues of COX2: COX2a and COX2b [32]. COX enzymes can produce prostaglandins in multiple cell types including epithelial cells, endothelial cells and fibroblasts, but infiltrating innate immune cells are the major source of these lipid signals during inflammation, including both macrophages [36] and neutrophils [11]. We find that both copies of COX2, but not COX1, are expressed in macrophages or

neutrophils, suggesting that phagocytes mainly deploy COX2-mediated responses in zebrafish larvae. In line with this, F0 crispant larvae in which *ptgs2a* and *2b* have been targeted but in which *ptgs1* is intact have impaired immune control of *A. fumigatus* infection. However, we cannot rule out an additional role of other cell types, such as epithelial cells, in initiating COX signaling in response to *A. fumigatus*, which could be mediated via COX1, COX2, or both.

COX enzymes catalyze the main regulatory step of prostaglandin synthesis: conversion of arachidonic acid to prostaglandin H_2 (PGH_2). PGH_2 is then converted to one of the four major types of prostaglandins, prostaglandin E_2 (PGE_2), prostaglandin D_2 (PGD_2), prostaglandin I_2 (PGI_2) and prostaglandin $F_{2\alpha}$ ($PGF_{2\alpha}$) via different synthases. Perhaps the most studied prostaglandin is PGE_2, due to its paradoxical immunomodulatory effects [37]. Membrane-bound (mPges) or cytosolic (cPges) PGE_2 synthases convert PGH_2 to PGE_2. cPges is functionally coupled with COX1 and responsible for constitutive PGE_2, while COX2-mPges is inducible in response to inflammatory stimuli [38,39]. In the current study, *mpges* was only detected in macrophages, suggesting macrophages may initiate PGE_2 signaling. Once released, PGE_2 signals via four different receptors, EP1-EP4 which have different affinities for PGE_2, and activate different downstream effects [26]. We find that pharmacological inhibition of EP2 leads to impaired control of fungal growth and increased susceptibility of the larval host at a rate similar to COX inhibition. At least one EP2 receptor gene (*ep2a* or *ep2b*) is expressed in both macrophages and neutrophils in larvae. Determining the specific role of each COX enzyme, PGE_2 synthase, and EP receptor in each cell type in response to *A. fumigatus* is complicated in zebrafish due to the presence of a teleost genome duplication that led to multiple copies of these genes [40], but should be the subject of future studies.

The decreased larval host survival that we observe when COX-PGE_2 signaling is inhibited is due to decreased phagocyte control of *A. fumigatus* spore germination and hyphal growth. In invasive aspergillosis, it is this hyphal growth that can penetrate into host tissues and cause organ damage and mortality. However, spore germination is a 'double-edged sword'—while it is required for fungal growth and pathogenesis, it also causes unmasking of fungal PAMPs and activation of immune responses [41]. As a result, in some infection scenarios, increased germination actually leads to better host survival. For example, *irf8*^{−/−} larval zebrafish that lack macrophages and have an excess of neutrophils clear infections with a fast-germinating CEA10 strain of *A. fumigatus* at a higher rate than wild-type larvae [20]. This specific host-pathogen interaction does not represent a "normal" *A. fumigatus* infection in which only a percentage of the spores present germinate in the presence of macrophages [20]. In these "normal" scenarios neutrophils take longer to respond and a slight decrease in immune control of fungal germination rate or hyphal growth rate will allow the infection to cause tissue destruction and death. However, we did use this *irf8*^{−/−} host infected with CEA10 to specifically measure the requirement for COX signaling in neutrophil killing of *A. fumigatus* hyphae. We find that when COX enzymes are inhibited, neutrophil-mediated CFU clearance is not significantly affected. These experiments also demonstrated that COX signaling is important for immune responses to the CEA10 strain as well as the Af293 strain used in the majority of our study.

We report here that PGE_2 signaling, specifically through the EP2 receptor, promotes phagocyte control of *A. fumigatus* invasive hyphal growth, but the cellular mechanisms upstream and downstream of this signaling in larval zebrafish are not yet determined. Treatment with a COX2 inhibitor was previously found to cause higher fungal burdens in *A. fumigatus*-infected mice [42]. Garth *et al.* found that signaling through the IL-33 receptor inhibits PGE_2 production and inhibits fungal clearance in the infected lung [42]. The cytokines IL-17A and IL-22 were also decreased in mice with lower levels of PGE_2, suggesting that these signals may act downstream of PGE_2 to coordinate the immune response [42,43]. Zebrafish have homologs for both *il22* and *il17a*, and *il22* mRNA expression is induced upon fungal infection in adult

zebrafish [44], but their roles in fungal infections in larval zebrafish are unknown. It is worth noting that these cytokines are thought to be primarily expressed by T cells, which are not yet developed in larval zebrafish, and our results demonstrate that COX-PGE$_2$ signaling also promotes immune responses to *A. fumigatus* infection in the absence of functional adaptive immunity.

We do not yet know what downstream effector mechanisms are activated in neutrophils and macrophages by COX signaling to target fungal growth. Prostaglandins can mediate endothelial cell permeability and facilitate immune cell infiltration, but we observe no difference in phagocyte recruitment when COX enzymes are inhibited [6,45,46]. Prostaglandins can also regulate extracellular killing mechanisms in phagocytes such as reactive oxygen species (ROS) production, neutrophil degranulation, and extracellular trap (ET) formation [47–49]. Further testing is required to determine if these mechanisms are enhanced by COX signaling during infection with *A. fumigatus*.

In contrast, it was previously reported that PGE$_2$ suppresses phagocytosis and microbial killing of fungal pathogens such as *P. brasiliensis* [12], *C. albicans* [13] and *C. neoformans* [14]. These differences underline the idea that PGE$_2$ can have both pro- or anti-inflammatory functions, can differentially impact diverse fungi, and that PGE$_2$ levels must be tightly controlled during infection to promote infection clearance. PGE$_2$ binds to EP2 with low affinity and generally evokes pro-inflammatory responses while it binds to EP4 with high affinity and activates anti-inflammatory responses [26]. In line with this idea, PGE$_2$ can drive resolution of inflammatory phenotypes through EP4 in zebrafish larvae during injury [28]. However, our data demonstrate that PGE$_2$-EP4 may also partially contribute to immune cell-mediated fungal growth control during *A. fumigatus* infection rather than inhibiting immune activation. PGE$_2$ levels, and eicosanoid levels in general, must be tightly controlled during infection, and an eicosanoid imbalance in either direction is known to increase pathogenesis of mycobacterial infections in zebrafish, mice, and humans [50–52].

Fungal species can also synthesize their own lipid signaling molecules to modulate pathogenesis and immune responses [53,54]. For instance, *Cryptococcus neoformans* strains deficient in eicosanoid production have intracellular growth defects, which can be reversed by addition of exogenous PGE$_2$ in a zebrafish larvae model [27]. *A. fumigatus* PpoA and PpoC enzyme activity can produce prostaglandins and similar bioactive oxylipins that can affect *Aspergillus* virulence and development [24] and phagocytosis of conidia [55]. However, we find that *A. fumigatus* Ppo enzymes do not affect fungal virulence in this larval zebrafish infection model, and that indomethacin treatment does not alter *A. fumigatus* spore germination *in vitro*. Additionally, while a previous study showed that exogenous PGE$_2$ inhibited pigment formation in *A. fumigatus* hyphae which could affect invasive hyphal growth [24], we do not find any direct effect of PGE$_2$ on *A. fumigatus* germination *in vitro*.

Overall, PGE$_2$ signaling must be well-orchestrated to elicit the desired anti- or pro-inflammatory effects. Hematopoietic stem cell transplant patients who are at high risk of developing IA harbor elevated levels of PGE$_2$ [56], suggesting that modulating PGE$_2$ or the downstream effects of PGE$_2$ signaling may be a possible target for increasing control of these infections in patients. Host-directed therapy to modulate PGE$_2$ levels during infection has also been suggested as a possible treatment for *Mycobacterium tuberculosis* infection [50]. This study provides a first step towards understanding the function of this signaling in immune-mediated control of *A. fumigatus* infection.

Materials and methods

Ethics statement

Adult and larval zebrafish were maintained and handled according to protocols approved by the Clemson University Institutional Animal Care and Use Committee (AUP2018-070,

AUP2019-012, and AUP2019-032). Buffered tricaine was used for anesthesia prior to any experimental manipulation of larvae. Adult zebrafish were euthanized with buffered tricaine and zebrafish embryos and larvae were euthanized at 4˚C.

Zebrafish lines and maintenance

Zebrafish adults were maintained at 28˚C at 14/10 hr light/dark cycles. All mutant and transgenic fish lines used in this study are listed in Table 1 and were maintained in the AB background. Upon natural spawning, embryos were collected and maintained in E3 medium with methylene blue at 28˚C. Embryos were manually dechorionated and anesthetized in 0.3 mg/mL buffered tricaine prior to any experimental manipulations. Larvae used for imaging were exposed to 200 μM N-phenylthiourea (PTU) starting at 24 hpf to inhibit pigment formation. Transgenic larvae were screened for fluorescence prior to experimentation. The *irf8* mutant line was maintained by outcrossing. *irf8*^{+/-} adults with fluorescent neutrophils (*Tg(mpx:mCherry)*) were in-crossed to generate *irf8*^{+/+}, *irf8*^{+/-} and *irf8*^{-/-} larvae, and these larvae were screened for a high number of neutrophils to select *irf8*^{-/-} individuals [57]. Genotypes were additionally confirmed at the end of the experiment where possible.

Aspergillus fumigatus strains

Most experiments used Af293-derived strains TBK1.1 expressing YFP [19] or TBK5.1 expressing mCherry [20]. Both of these strains behave like the parental Af293 strain in larval zebrafish [20]. To test neutrophil-mediated killing, GFP-expressing TFYL49.1 [62] which was derived from the faster germinating CEA10 strain was used.

A Δ*ppoA*, Δ*ppoB*, Δ*ppoC* triple-mutant strain (Δ*ppo*, TMN31.10) was used to test the role of fungal oxylipins. In these experiments the control comparison strain used was wild-type Af293. Briefly, a previously published Af293 Δ*ppoC pyrG1* strain TDWC3.4 [24] was used as the parental strain in which *ppoA* and *ppoB* were subsequently deleted, using the *A. parasiticus pyrG* marker and recyclable hygromycin resistance marker *hph* [63], respectively. All primers used for strain construction and confirmation are listed in S1 Table. DNA transformation constructs were created through double-joint PCR using published protocols [64]. Protoplast generation and transformation were performed according to the previously published protocol [65]. All transformants were first screened through PCR for incorporation of the construct and absence of the *ppo* gene. Southern blotting followed by hybridization of αP^{32}-dCTP labeled 5′ and 3′ flank regions were used to confirm transformants with single integration (S2 Fig). The *ppoA* deletion construct was amplified from pDWC4.2 (GF ppoA del Cassette F and GF ppoA del Cassette R) and used to transform TDWC3.4, resulting in the prototroph Af293 Δ*ppoC* Δ*ppoA* TMN20. A deletion cassette for *ppoB* was constructed by fusing ~1 kb 5′ and 3′ flanking regions of the gene with the recyclable hygromycin B resistance gene *hph* from

Table 1. Zebrafish lines used in this study.

Zebrafish line	Reference
irf8^{-/-}	[57]
Tg(mpeg1:H2B-GFP)	[58]
Tg(mpeg1:H2B-mCherry)	[59]
Tg(mfap4:mTurquoise2)	[60]
Tg(lyz:BFP)	[20]
Tg(mpx:mCherry)	[61]
Tg(mpx:mCherry-2A-rac2D57N)	[30]

https://doi.org/10.1371/journal.ppat.1010040.t001

pSK529. *ppoB* deletion cassette was used to transform TMN20.11, resulting in the *ppo* triple deletion mutant TMN31. TMN31 transformants were subsequently grown on minimal medium with 0.1% xylose to recycle the hygromycin B marker.

Spore preparation for injections

For injection preparation, 10^6 spores were spread on solid glucose minimal media (GMM) 10 cm plates and grown at 37˚C for 3–4 days. Spores were harvested by scraping using a disposable L-spreader and sterile water with 0.01% Tween. This spore suspension was passed through two layers of sterile miracloth into a 50 mL conical tube and topped to 50 mL. Spores were pelleted by centrifugation at 900 g for 10 min. The pellet was resuspended and washed in 50 mL of sterile PBS. The spores were again pelleted, resuspended in 5 mL of PBS, and filtered through another two layers of miracloth into a new conical tube. Spore concentration was enumerated using a hemocytometer. A final spore suspension of 1.5×10^8/ mL was made in PBS and stored at 4˚C for up to ~1 month.

Live-dead spore labeling

Spores of *A. fumigatus* strain TBK1.1 were coated with AlexaFluor546 as described previously [20,33]. Briefly, isolated spores were incubated with biotin-XX, SSE (Molecular Probes) in the presence of 0.05 M $NaHCO_3$ at 4˚C for 2 hours. Spores were pelleted, washed first with 100 mM Tris-HCl at pH 8.0 to deactivate free-floating biotin and next with PBS, followed by incubation with streptavidin-AlexaFluor546 (Invitrogen). Spore concentration was enumerated and resuspended in PBS at 1.5×10^8/ mL. Labeling was confirmed with fluorescence microscopy prior to injections.

Zebrafish hindbrain microinjections

Larvae were injected with spores as described previously [16]. Prepared spore suspensions at 1.5×10^8/ mL were mixed at 2:1 with filter-sterilized 1% phenol red to achieve a final spore concentration of 1×10^8/ mL. Injection plates were made with 2% agarose in E3 and coated with filter-sterilized 2% bovine serum albumin (BSA) prior to injections. Anesthetized 2 days post fertilization (dpf) larvae were placed on the agarose on their lateral side. A microinjection setup supplied with pressure injector, micromanipulator, micropipet holder, footswitch and back pressure unit (Applied Scientific Instrumentation) was used to inject 30–50 spores into the hindbrain ventricle of each larva. Larvae were injected with PBS as a mock-infection control. After injections, larvae were rinsed at least twice with E3 without methylene blue to remove tricaine and any free spores and were transferred to 96-well plates for survival and CFU experiments and to 48-well plates for imaging experiments.

Clodronate liposome injections

Tg(mpeg1:H2B-GFP) larvae at 1.5 dpf were manually dechorionated and screened for GFP expression. 50 µL of clodronate or PBS liposomes (Liposoma) was mixed with 5 µL of filter-sterilized 1% phenol red and 2 nL was intravenously injected into the caudal vein plexus of GFP-positive larvae. After 24 hours, depletion of macrophages was confirmed by loss of GFP signal by screening with a fluorescent zoomscope (Zeiss SteREO Discovery.V12 PentaFluar with Achromat S 1.0x objective) prior to *A. fumigatus* infections.

Morpholino injections

A *pu.1* (*spi1b*) morpholino oligonucleotide (MO) was previously published and validated (5'-GATATACTGATACTCCATTGGTGGT-3') (ZFIN MO1-spi1b) [29] (GeneTools). Stock

solutions were made by resuspension in water to 1 mM and kept at 4˚C. For injections, the stock was diluted to 0.5 mM in water with 0.1% filter-sterilized phenol red and 0.5X CutSmart Buffer (New England Biolabs). A standard control MO (GeneTools) at 0.5 mM was used as an injection control. 3 nl of injection mix was injected into the yolk of 1–2 cell stage embryos. Efficacy of *pu.1* knockdown was determined by injecting MO into a macrophage-labeled zebrafish line and larvae were checked for fluorescence expression prior to *A. fumigatus* infections.

CRISPR gRNA design and injections

Guide RNAs (gRNAs) were designed to target both copies of COX2, *ptgs2a* and *ptgs2b*, and two control GFP-targeting gRNAs using the CHOPCHOP web-based program [66–68]. gRNAs target predicted heme-binding sites located in exon 7 of both *ptgs2* genes [32]. Target sequences are (from 5'-3') *ptgs2a*: AATTCAATACCCTGTATCAC, *ptgs2b*: GTTATGTTCAC GCAGCCAGA, *gfp1*: CAACTACAAGACCCGCGCCG, and *gfp2*: GACGTAGCCTTCGGG CATGG. DNA templates for gRNAs were synthesized via a cloning-free oligo annealing and extrension method. Gene-specific oligos included T7 promoter sequence, target sequence, and overlap sequence to pair with a constant oligo. The constant oligo (5'-AAAAGCACCGACT CGGTGCCACTTTTTCAAGTTGATAACGGACTAGCCTTATTTTAACTTGC TATTTC TAGCTCTAAAAC -3') encodes the constant region of the gRNA that binds to Cas9. Oligos were annealed and T4 DNA polymerase (New England Biolabs) was used to fill in remaining bases. gRNAs were then *in vitro* transcribed with T7 RNA polymerase (New England Biolabs), treated with DNase I (New England Biolabs), and purified using Monarch RNA cleanup kit (New England Biolabs). The embryo injection mix consisted of 195 ng of *ptgs2a* gRNA and 300 ng of *ptgs2b* gRNA with 1 μg of Cas9 protein (PNA Bio) in a total volume of 3.9 μL, and the same concentrations of the two gRNAs targeting *gfp* in a control mix. 1–2 nL of the mix was injected into the yolk of 1-cell stage embryos. CRISPR F0 larvae were injected with spores of *A. fumigatus* strain TBK1.1 at 2 dpf and were imaged at 3 dpi. Genomic DNA was extracted from whole larvae at 2 dpf using 50 mM NaOH and the efficacy of gRNA was tested by PCR. Only replicates with successful cutting were included in the analysis. The primers used are listed in S1 Table.

Drug treatments

Infected larvae were exposed to the pan-COX inhibitor indomethacin (Sigma-Aldrich) at 10 μM, COX1 inhibitor SC560 (Cayman Chemical) at 5 μM, COX2 inhibitor meloxicam (Cayman Chemical) at 15 μM, EP2 receptor antagonist AH6809 (Cayman Chemical) at 5 μM or EP4 receptor antagonist AH23848 (Cayman Chemical) at 10 μM. These drugs were previously used in zebrafish larvae [21–23,27,28]. The indomethacin concentration used was based on published results. For all other drugs, multiple concentrations were tested and the highest concentration of each drug that did not cause lethality or edema in uninfected larvae was used. 1000X stock solutions were made in DMSO and 0.1% DMSO was used as a vehicle control. After rinsing infected larvae, pre-mixed E3 with drug was added to dishes containing larvae. For survival and CFU assays, larvae were transferred to 96-well plates, one larva/well in 200 μL of drug/vehicle solution. For imaging experiments, larvae were transferred to 48-well plates with 500 μL of solution. All larvae were kept in the same drug solution for the entirety of the experiment unless otherwise noted.

PGE$_2$ rescue injections

A stock solution of 10 mM PGE$_2$ (Cayman Chemical) was made in DMSO [23,27]. Prior to injection, the stock was diluted 100X in PBS and 1 μL was mixed with 9 μL of 1% phenol red

for a final concentration of 10 μM. Wild-type larvae were injected with *A. fumigatus* and exposed to 10 μM indomethacin, 5 μM AH23848 or DMSO vehicle control in 10 mL of E3 in 60 mm petri dishes. At 1 dpi, larvae were anesthetized and injected with 1 nL of 10 μM PGE$_2$ or 0.1% DMSO into the hindbrain. After injections, indomethacin or DMSO control treatments were renewed, and larvae were transferred to 96-well plates for survival and 6-well plates for imaging experiments.

CFU counts

Single larvae were placed in 1.7 mL microcentrifuge tubes in 90 μl PBS containing 1 mg/mL ampicillin and 0.5 mg/mL kanamycin, homogenized in a tissue lyser (Qiagen) at 1800 oscillations/min (30 Hz) for 6 min and spun down at 17000 g for 30 seconds. The whole suspension was spread on a GMM plate and incubated for 3 days at 37˚C and the number of fungal colonies were counted. For all survival experiments, 8 larvae from each condition were plated immediately after injection to confirm actual injection dose and these numbers are reported in all figure legends. For CFU experiments to monitor fungal burden over time, 8 larvae were plated for each condition, each day and CFU counts were normalized to the average initial injection dose for that condition and graphed as percent initial spore burden.

COX activity assay

Total COX activity was measured in infected larvae using a COX activity assay kit (Cayman Chemical). Larvae injected with *A. fumigatus* spores or PBS mock-infection were anesthetized and flash frozen in liquid nitrogen at 2, 3, and 4 dpi and were stored at -80˚C until the assay was performed. A total of 200 larvae were used per condition per dpi. Just before the assay, larvae were homogenized in 400 μl of 0.1M Tris-HCl (pH–7.5) spiked with 0.1 mM phenylmethanesulfonyl fluoride (PMSF). This crude extract was centrifuged at 10000 g for 15 mins at 4˚C and the supernatant was used to perform the assay. Aliquots of 150 μl of the samples were boiled in a heat block for 5 mins and used as a background control. The assay was performed according to the manufacturer's instructions. Briefly, 1X assay buffer was added to a 96-well plate, followed by hemin, samples, and a standard control. The colorimetric solution and the arachidonic substrate acid were added, and absorbance in each well was measured at 590 nm using a plate reader (BioTek). COX activity levels were calculated according to the manufacturer's instructions. Triplicate technical replicates were done for each sample for each experimental replicate.

FACS and RT-PCR

Tg(mpeg1:H2B-GFP) and *Tg(mpx:mCherry)* larvae were used to sort macrophages and neutrophils. A total of 200–300 larvae at 3 dpf were anesthetized and deyolked by pipetting up and down with a P100. Deyolked larvae were incubated with 5 ml PBS containing 0.25% trypsin (Life Technologies) and 1 mM EDTA for 60 min at 28˚C. The reaction was stopped by adding 1 mM CaCl$_2$ and samples were strained through a 40 μm cell filter. Cells were centrifuged at 736 g at 4˚C for 3 mins and resuspended in 0.5–1 mL of ice-cold PBS containing 10% FBS (Life Technologies) and kept on ice until sorting. Cell sorting was performed using a S3E cell sorter (Bio Rad), cells were collected in 500 μL of TRIzol (Invitrogen), and RNA was extracted using glycogen as a carrier. RNA extracted from 20 whole larvae of matching age was used as a control. 500 ng RNA was incubated with DNaseI (New England Biolabs) to remove any genomic DNA and cDNA synthesis was carried out using iScript RT Supermix with oligo dT (Bio-Rad). Undiluted cDNA was used as template for PCR (40 cycles) using GoTaq G2 green master mix (Promega). *rps11* [69] was amplified as a positive control. To test the purity of sorting,

liver-specific *fabp1*, macrophage-specific *csf1ra* [70], and neutrophil-specific *mpx* [70] genes were amplified. Primers are listed in S1 Table.

Live imaging

For daily imaging, individual larvae were removed from 48-well plates, anesthetized in tricaine and transferred to a zWEDGI device [71,72]. For AH6809-exposed larvae and CRISPR F0 larvae, the same protocol was used, but imaged only once at 3 dpi. Larvae were imaged using a Zeiss Cell Observer Spinning Disk confocal microscope on a Axio Obsever 7 microscope stand with a confocal scanhead (Yokogawa CSU-X) and a Photometrics Evolve 512 EMCCD camera. A Plan-Apochromat 20x objective (0.8 NA) and ZEN software were used to acquire Z-stack images of the hindbrain area with 5 μm distance between slices. After imaging, larvae were rinsed with 200 μM PTU in E3 and put back in the same well [16]. For single time point imaging at 2 or 3 dpi, larvae were either loaded into a zWEDGI device or mounted in 1% low-melting point agarose (Fisher BioReagents) in a 35mm glass-bottom dish (Greiner) and oriented laterally. Images were acquired using the same spinning disk confocal microscope with an EC Plan-Neofluar 40x objective (0.75 NA) with either 2.5 μm or 5 μm distance between slices.

Image analysis

All images were analyzed using Image J/Fiji [73]. Presence of germination and invasive hyphae were manually analyzed. Any kind of hyphal growth, whether single or branched was considered an incidence of germination, while the presence of branched hyphae was considered an incidence of invasive hyphae. Maximum intensity projections were used to measure the 2D fungal area after thresholding the fluorescent intensity. The number of recruited phagocytes were counted across z-stacks using the Cell Counter plugin. For 2D phagocyte cluster area, the polygon selection tool was used to select and measure the area of macrophage cluster from maximum intensity projection of z-stacks. Images from the same experiments were used to quantify incidence of germination and invasive hyphae, fungal area, and phagocyte recruitment. To quantify live versus dead spores, images were blinded and processed with bilinear interpolation to increase pixel density two-fold. Cell Counter was used to manually count the number of live and dead spores in z-slices. For AH6809 exposure, PGE_2 rescue and CRISPR F0 imaging experiments, all images were blinded prior to analysis. All displayed images were processed in Fiji with bilinear interpolation to increase pixel density two-fold and are displayed as maximum intensity projections of z-stacks. Live versus dead spore images were additionally processed with a gaussian blur (radius = 1) to reduce noise.

Aspergillus fumigatus in vitro germination assay

$1 X 10^6$ TBK1.1 spores were inoculated into a 15 mL conical tube containing 3 ml RPMI 1640 medium with HEPES (Gibco) containing 2% glucose in a 37°C shaker at 200 rpm in the presence of 10 μM indomethacin, 1 μM or 10 μM PGE_2 or DMSO vehicle control in triplicate. Every 2 hours, 10 μL of the spore suspension was pipetted on to a microscope slide with a cover glass and imaged under the same Zeiss spinning disk confocal microscope using a Plan-Apochromat 20x objective (0.8 NA). At least 10 fields were captured for each sample at each time point and imaging was continued until 8 hours post seeding. These images were blinded prior to analysis and the number of germinated and non-germinated spores were counted using the Fiji Cell Counter plugin.

Statistical analysis

For all experiments, unless stated otherwise, pooled data from at least three independent replicates were generated and total pooled Ns are given in each figure. Statistical analyses were performed using R version 4.1.0 and graphs were generated using GraphPad Prism version 7 (GraphPad Software). While the data are pooled from three or more independent replicates, the statistical analysis takes into account the variability within and between replicates and considers independent replicates as individual entities. Larval survival data and cumulative appearance of larvae with germination or invasive hyphae were analyzed by Cox proportional hazard regression. Calculated experimental P values and hazard ratios (HR) are displayed in each figure. HR defines how likely larvae in a particular condition will succumb to the infection compared to control larvae. Occasionally, the indomethacin drug lost efficacy and did not cause the previously observed and confirmed survival defect. Any such replicates were omitted from the final statistical analysis. CFU counts, spore killing, fungal area, phagocyte numbers and cluster area, and comparisons of day of onset of germination and invasive hyphae were analyzed with analysis of variance (ANOVA). For each condition, estimated marginal means (emmeans) and standard error (SEM) were calculated and pairwise comparisons were performed with Tukey's adjustment. The graphs of number of phagocytes, phagocyte cluster area and 2D fungal area over the infection period show values from individual larvae over time as individual lines, and bars represent pooled emmeans ± SEM. Data points in dot plots represent individual larvae and are color-coded based on replicate and bars represent pooled emmeans ± SEM. For single day imaging experiments, the total number of larvae with germination or invasive hyphae were compared using Fisher's Exact Test. Bars represent the percentage of larvae with each phenotype at 3 dpi. For the *in vitro* germination assay, data were pooled from two independent replicates, each consisting of three technical replicates. Graphs represent means ± SEM at each time point.

Supporting information

S1 Fig. Both cyclooxygenase-1 and -2 signaling contribute to survival of infected larvae. **(A, B)** Larvae were injected with TBK1.1 (Af293) *A. fumigatus* spores at 2 dpf and were exposed to (A) 5 μM SC560, (B) 15 μM meloxicam, or DMSO vehicle control. Survival was monitored for 7 days. Cox proportional hazard regression analysis was used to calculate P values and hazard ratios (HR). Data are pooled from three independent experiments, at least 19 larvae per condition, per replicate and the total larval N per condition is indicated in each figure. **(C)** Total cyclooxygenase activity of larvae injected with TBK1.1 (Af293) *A. fumigatus* spores or PBS mock-infection as detected by Cox activity assay kit. 200 infected larvae at 2, 3, and 4 dpi were homogenized, and bulk extracts were analyzed. Data are averaged from three independent experiments and P values calculated by ANOVA. Bars represent means ± SEM. Average injection CFUs: (A) 35, (B) 30, (C) 2 dpi = 57, 3 dpi = 62, 4 dpi = 64.
(TIF)

S2 Fig. Southern blot analyses of strains created in this study. Confirmation of **(A)** TMN20 Af293 *ΔppoC ΔppoA* double mutant and **(B)** TMN31 Af293 *ΔppoC ΔppoA ΔppoB* triple mutant. Restriction enzyme digestion, southern blotting and hybridization were performed as mentioned in the Materials and Methods. Double and triple *ppo* mutants were created in sequence. Hybridization of αP^{32}-dCTP labeled 5′ and 3′ flank regions were used to confirm transformants. The parental strain and the size of DNA fragments used to probe for southern blotting and hybridization are shown in each figure. P = parental strain; T = transformants.
(TIF)

S3 Fig. Survival of phagocyte-deficient larvae after PBS mock-infection. (A) Wild-type larvae injected with standard control MO or *pu.1* MO, **(B)** larvae injected with PBS liposomes or clodronate liposomes and **(C)** larvae with defective neutrophils (*mpx:rac2D57N*) or wild-type neutrophils were injected with PBS at 2 dpf. Survival was monitored in the presence of 10 μM indomethacin or DMSO vehicle control. Data are pooled from three independent experiments, at least 9 larvae per condition, per replicate and the total larval N per condition is indicated in each figure. Cox proportional hazard regression analysis was used to calculate P values and hazard ratios (HR).
(TIF)

S4 Fig. Expression COX-PGE$_2$ pathway genes in isolated macrophages and neutrophils. Larvae expressing GFP in macrophages (*Tg(mpeg1:H2B-GFP)*) or mCherry in neutrophils (*Tg (mpx:mCherry)*) were trypsinized and single cell suspensions were subjected to FACS. Two independent replicates were performed. **(A, B)** Gating used to isolate GFP-expressing macrophages (A) and mCherry expressing neutrophils (B). **(C, D)** RNA was extracted from sorted cells and RT-PCR was performed for the genes shown. (C) DNA gels for two replicates. W: whole larvae control, M: isolated macrophages, N: isolated neutrophils, -: negative controls. (D) Summary table of gene expression from both replicates. Presence of a band is represented by 1.
(TIF)

S5 Fig. Non-normalized CFU data in control and indomethacin-treated larvae. Wild-type larvae were injected with TBK1.1 (Af293) spores at 2 dpf, exposed to **(A)** 10 μM indomethacin or **(B)** DMSO vehicle control, and fungal burden was quantified by homogenizing and plating individual larvae for CFUs at multiple days post injection. Eight larvae per condition, per dpi, per replicate were quantified, and the number of CFUs at each dpi is represented. Each data point represents an individual larvae, color-coded by replicate. Bars represent means ± SEM from three individual replicates. Average injection CFUs: 27. This same data is normalized to the initial spore injection and presented in Fig 4.
(TIF)

S6 Fig. Indomethacin does not affect *A. fumigatus* spore germination *in vitro*. TBK1.1 (Af293) spores were inoculated into RPMI media in the presence of 10 μM indomethacin or DMSO vehicle control. Every 2 hours, an aliquot of spores was removed and scored for germination. Points represent pooled means ± SEM from two independent replicates.
(TIF)

S7 Fig. Representative images of categories of *A. fumigatus* hyphal growth. Wild-type larvae were injected with mCherry-expressing TBK5.1 (Af293) spores, exposed to 10 uM indomethacin or DMSO vehicle control and imaged at 1, 2, 3, and 5 dpi. Incidences of hyphal growth were scored a value of 1–4 depending on the extent of hyphae. Category 1: presence of one germ tube (white arrow). Category 2: presence of branched hyphae (open white arrow), yet small fungal bolus. Category 3: presence of spread-out invasive hyphae. Category 4: presence of severe invasive hyphae and tissue damage. Scale bars = 50 μm or 10 μm.
(TIF)

S8 Fig. Inhibition of EP2 receptor increases *A. fumigatus* spore germination in zebrafish larvae. Wild-type larvae were injected with mCherry-expressing TBK5.1 (Af293) spores and exposed to 5 μM AH6809 or DMSO vehicle control at 2 dpf. Larvae were imaged at 3 dpi and the percentage of larvae with germination and invasive hyphae was calculated. Data are pooled from three independent replicates, at least 11 larvae per condition, per replicate, P values

calculated by Fisher's Exact Test.
(TIF)

S9 Fig. Indomethacin does not significantly impair neutrophil-mediated clearance of *A. fumigatus* hyphae. Macrophage-deficient *irf8*$^{-/-}$ or control (*irf8*$^{+/+}$ or *irf8*$^{+/-}$) larvae were injected with *A. fumigatus* TFYL49.1 (CEA10) strain and treated with 10 μM indomethacin or DMSO vehicle control. **(A)** Fungal burden was monitored by homogenizing individual larvae and quantifying CFUs at 1 and 2 dpi. CFUs from *irf8*$^{-/-}$ were normalized to CFUs of *irf8*$^{+/+}$/*irf8*$^{+/-}$ at each dpi for each condition. Data were pooled from four independent replicates, 8 larvae per condition, per dpi, and P values calculated by ANOVA. **(B)** Larvae were monitored for survival. Data are pooled from five independent replicates, at least 8 larvae per condition, per replicate and the total larval N per condition is indicated. Cox proportional hazard regression analysis was used to calculate P values and hazard ratios (HR). Average injection CFUs: *irf8*$^{+/+}$/*irf8*$^{+/-}$ = 26, *irf8*$^{-/-}$ = 20.
(TIF)

S10 Fig. Pre-treatment with or exposure to higher concentrations of indomethacin causes toxicity in zebrafish larvae. Larvae were exposed to 10 μM or 20 μM indomethacin, or DMSO vehicle control at 1 dpf (1 day prior to injection) or at 2 dpf (immediately after injection) and survival was monitored for 7 days. Survival of larvae injected with **(A)** TBK1.1 (Af293) *A. fumigatus* spores, or **(B)** PBS mock-infection. Data are pooled from two independent experiments, at least 20 larvae per condition, per replicate and the total larval N per condition is indicated in each figure. (A) Average injection CFUs: 2 dpf treatment = 35, pre-treatment DMSO = 38, 10 μM indomethacin = 50, 20 μM indomethacin = 62.
(TIF)

S11 Fig. Efficiency of CRISPR gRNA. (A) A schematic showing the structure of *ptgs2* genes and the target sites for gRNA binding. **(B)** Wild-type larvae were injected with gRNAs targeting both *ptgs2a* and *ptgs2b* or *gfp* control. Genomic DNA from 4 individual larvae from each group was used in PCR reactions with primers flanking the gRNA target sites. Each lane represents PCR amplification of an individual larva.
(TIF)

S12 Fig. PGE$_2$ injection does not alter phagocyte recruitment or rescue survival of neutrophil-defective larvae. At 2 dpf, larvae were injected with TBK5.1 (Af293), followed by injection of 10 μM PGE$_2$ or DMSO vehicle control at 3 dpf (1 dpi). **(A, B)** Macrophage nuclear-labeled *Tg(mpeg1:H2B-GFP)* and neutrophil-labeled *Tg(lyz:BFP)* larvae were imaged at 3 dpi and the number of (A) macrophages and (B) neutrophils were enumerated. Data are pooled from three independent replicates, at least 8 larvae per condition, per replicate. Each data point represents an individual larva, color-coded by replicate. Bars represent pooled emmeans ± SEM and P values were calculated by ANOVA. **(C)** Survival of injected and treated neutrophil-defective larvae (*mpx:rac2D57N*) was monitored. Cox proportional hazard regression analysis was used to calculate P values and hazard ratios (HR). Data are pooled from three replicates, at least 23 larvae per condition, per replicate. Average injection CFUs: 49.
(TIF)

S1 Table. Primers used in this study.
(DOCX)

Acknowledgments

other transgenic zebrafish lines. We thank members of the Rosowski Lab and Keller Lab for helpful discussions. We thank Justin Scott at the Clemson University Light Imaging Facility for assistance with FACS. We thank John Smink and the Aquatic Animal Research Laboratory for assistance with fish system maintenance and for providing the microinjection set-up for single-cell embryo injections.

Author Contributions

References

1. Latge JP. Aspergillus fumigatus and aspergillosis. Clinical microbiology reviews. 1999; 12(2):310–50. https://doi.org/10.1128/CMR.12.2.310 PMID: 10194462

2. Baddley JW. Clinical risk factors for invasive aspergillosis. Medical mycology. 2011; 49 Suppl 1:S7–S12. https://doi.org/10.3109/13693786.2010.505204 PMID: 20718606

3. Denning DW. Invasive aspergillosis. Clinical infectious diseases. 1998; 26(4):781–803. https://doi.org/10.1086/513943 PMID: 9564455

4. Lin SJ, Schranz J, Teutsch SM. Aspergillosis case-fatality rate: systematic review of the literature. Clinical infectious diseases. 2001; 32(3):358–66. https://doi.org/10.1086/318483 PMID: 11170942

5. Gregg KS, Kauffman CA. Invasive Aspergillosis: Epidemiology, Clinical Aspects, and Treatment. Seminars in respiratory and critical care medicine. 2015; 36(5):662–72. https://doi.org/10.1055/s-0035-1562893 PMID: 26398533

6. Ricciotti E, FitzGerald GA. Prostaglandins and inflammation. Arteriosclerosis, thrombosis, and vascular biology. 2011; 31(5):986–1000. https://doi.org/10.1161/ATVBAHA.110.207449 PMID: 21508345

7. Funk CD. Prostaglandins and leukotrienes: advances in eicosanoid biology. Science (New York, NY). 2001; 294(5548):1871–5. https://doi.org/10.1126/science.294.5548.1871 PMID: 11729303

8. Smith WL, DeWitt DL, Garavito RM. Cyclooxygenases: structural, cellular, and molecular biology. Annual review of biochemistry. 2000; 69:145–82. https://doi.org/10.1146/annurev.biochem.69.1.145 PMID: 10966456

9. Vane JR. Inhibition of Prostaglandin Synthesis as a Mechanism of Action for Aspirin-like Drugs. Nature New Biology. 1971; 231(25):232–5. https://doi.org/10.1038/newbio231232a0 PMID: 5284360

10. Williams CS, Mann M, DuBois RN. The role of cyclooxygenases in inflammation, cancer, and development. Oncogene. 1999; 18(55):7908–16. https://doi.org/10.1038/sj.onc.1203286 PMID: 10630643

11. Tilley SL, Coffman TM, Koller BH. Mixed messages: modulation of inflammation and immune responses by prostaglandins and thromboxanes. Journal of Clinical Investigation. 2001; 108(1):15–23. https://doi.org/10.1172/JCI13416 PMID: 11435451

12. Bordon AP, Dias-Melicio LA, Acorci MJ, Calvi SA, Serrão Peraçoli MT, Victoriano de Campos Soares AM. Prostaglandin E2 inhibits Paracoccidioides brasiliensis killing by human monocytes. Microbes and Infection. 2007; 9(6):744–7. https://doi.org/10.1016/j.micinf.2007.02.019 PMID: 17400014

13. Serezani CH, Kane S, Medeiros AI, Cornett AM, Kim SH, Marques MM, et al. PTEN directly activates the actin depolymerization factor cofilin-1 during PGE2-mediated inhibition of phagocytosis of fungi. Science signaling. 2012; 5(210):ra12. https://doi.org/10.1126/scisignal.2002448 PMID: 22317922

14. Shen L, Liu Y. Prostaglandin E2 blockade enhances the pulmonary anti-Cryptococcus neoformans immune reaction via the induction of TLR-4. International Immunopharmacology. 2015; 28(1):376–81. https://doi.org/10.1016/j.intimp.2015.06.026 PMID: 26122137

15. Rosowski EE. Illuminating Macrophage Contributions to Host-Pathogen Interactions In Vivo: the Power of Zebrafish. Infection and immunity. 2020; 88(7). https://doi.org/10.1128/IAI.00906-19 PMID: 32179583

16. Thrikawala S, Rosowski EE. Infection of Zebrafish Larvae with Aspergillus Spores for Analysis of Host-Pathogen Interactions. Journal of visualized experiments. 2020(159). https://doi.org/10.3791/61165 PMID: 32478760

17. Traver D, Herbomel P, Patton EE, Murphey RD, Yoder JA, Litman GW, et al. The Zebrafish as a Model Organism to Study Development of the Immune System. Advances in Immunology. 2003; 81:254–330. PMID: 14711058

18. Herbomel P, Thisse B, Thisse C. Ontogeny and behaviour of early macrophages in the zebrafish embryo. Development. 1999; 126(17):3735–45. https://doi.org/10.1242/dev.126.17.3735 PMID: 10433904

19. Knox BP, Deng Q, Rood M, Eickhoff JC, Keller NP, Huttenlocher A. Distinct innate immune phagocyte responses to Aspergillus fumigatus conidia and hyphae in zebrafish larvae. Eukaryotic cell. 2014; 13 (10):1266–77. https://doi.org/10.1128/EC.00080-14 PMID: 24879123

20. Rosowski EE, Raffa N, Knox BP, Golenberg N, Keller NP, Huttenlocher A. Macrophages inhibit Aspergillus fumigatus germination and neutrophil-mediated fungal killing. PLoS pathogens. 2018; 14(8): e1007229. https://doi.org/10.1371/journal.ppat.1007229 PMID: 30071103

21. Tyrkalska SD, Candel S, Angosto D, Gomez-Abellan V, Martin-Sanchez F, Garcia-Moreno D, et al. Neutrophils mediate Salmonella Typhimurium clearance through the GBP4 inflammasome-dependent production of prostaglandins. Nature communications. 2016; 7:12077. https://doi.org/10.1038/ncomms12077 PMID: 27363812

22. Jin D, Ni TT, Sun J, Wan H, Amack JD, Yu G, et al. Prostaglandin signalling regulates ciliogenesis by modulating intraflagellar transport. Nature cell biology. 2014; 16(9):841–51. https://doi.org/10.1038/ncb3029 PMID: 25173977

23. Lewis A, Elks PM. Hypoxia Induces Macrophage tnfa Expression via Cyclooxygenase and Prostaglandin E2 in vivo. Frontiers in immunology. 2019; 10:2321. https://doi.org/10.3389/fimmu.2019.02321 PMID: 31611882

24. Tsitsigiannis DI, Bok JW, Andes D, Nielsen KF, Frisvad JC, Keller NP. Aspergillus cyclooxygenase-like enzymes are associated with prostaglandin production and virulence. Infection and immunity. 2005; 73 (8):4548–59. https://doi.org/10.1128/IAI.73.8.4548-4559.2005 PMID: 16040966

25. Kupfahl C, Tsikas D, Niemann J, Geginat G, Hof H. Production of prostaglandins, isoprostanes and thromboxane by Aspergillus fumigatus: identification by gas chromatography-tandem mass spectrometry and quantification by enzyme immunoassay. Molecular immunology. 2012; 49(4):621–7. https://doi.org/10.1016/j.molimm.2011.10.010 PMID: 22118804

26. Hata AN, Breyer RM. Pharmacology and signaling of prostaglandin receptors: multiple roles in inflammation and immune modulation. Pharmacol Ther. 2004; 103(2):147–66. https://doi.org/10.1016/j.pharmthera.2004.06.003 PMID: 15369681

27. Evans RJ, Pline K, Loynes CA, Needs S, Aldrovandi M, Tiefenbach J, et al. 15-keto-prostaglandin E2 activates host peroxisome proliferator-activated receptor gamma (PPAR-gamma) to promote Cryptococcus neoformans growth during infection. PLoS pathogens. 2019; 15(3):e1007597. https://doi.org/10.1371/journal.ppat.1007597 PMID: 30921435

28. Loynes CA, Lee JA, Robertson AL, Steel MJ. PGE(2) production at sites of tissue injury promotes an anti-inflammatory neutrophil phenotype and determines the outcome of inflammation resolution in vivo. Science advances. 2018; 4(9):eaar8320. https://doi.org/10.1126/sciadv.aar8320 PMID: 30191175

29. Rhodes J, Hagen A, Hsu K, Deng M, Liu TX, Look AT, et al. Interplay of pu.1 and gata1 determines myelo-erythroid progenitor cell fate in zebrafish. Developmental cell. 2005; 8(1):97–108. https://doi.org/10.1016/j.devcel.2004.11.014 PMID: 15621533

30. Deng Q, Yoo SK, Cavnar PJ, Green JM, Huttenlocher A. Dual roles for Rac2 in neutrophil motility and active retention in zebrafish hematopoietic tissue. Developmental cell. 2011; 21(4):735–45. https://doi.org/10.1016/j.devcel.2011.07.013 PMID: 22014524

31. Knox BP, Blachowicz A, Palmer JM, Romsdahl J, Huttenlocher A, Wang CC, et al. Characterization of Aspergillus fumigatus Isolates from Air and Surfaces of the International Space Station. mSphere. 2016; 1(5). https://doi.org/10.1128/mSphere.00227-16 PMID: 27830189

32. Ishikawa TO, Griffin KJ, Banerjee U, Herschman HR. The zebrafish genome contains two inducible, functional cyclooxygenase-2 genes. Biochemical and biophysical research communications. 2007; 352 (1):181–7. https://doi.org/10.1016/j.bbrc.2006.11.007 PMID: 17112475

33. Jhingran A, Mar KB, Kumasaka DK, Knoblaugh SE, Ngo LY, Segal BH, et al. Tracing conidial fate and measuring host cell antifungal activity using a reporter of microbial viability in the lung. Cell reports. 2012; 2(6):1762–73. https://doi.org/10.1016/j.celrep.2012.10.026 PMID: 23200858

34. Langenbach R, Morham SG, Tiano HF, Loftin CD, Ghanayem BI, Chulada PC, et al. Prostaglandin synthase 1 gene disruption in mice reduces arachidonic acid-induced inflammation and indomethacin-induced gastric ulceration. Cell. 1995; 83(3):483–92. https://doi.org/10.1016/0092-8674(95)90126-4 PMID: 8521478

35. McAdam BF, Mardini IA, Habib A, Burke A, Lawson JA, Kapoor S, et al. Effect of regulated expression of human cyclooxygenase isoforms on eicosanoid and isoeicosanoid production in inflammation. The Journal of clinical investigation. 2000; 105(10):1473–82. https://doi.org/10.1172/JCI9523 PMID: 10811855

36. Harizi H. The Immunobiology of Prostanoid Receptor Signaling in Connecting Innate and Adaptive Immunity. BioMed research international. 2013; 2013:683405. https://doi.org/10.1155/2013/683405 PMID: 24024207

37. Kalinski P. Regulation of immune responses by prostaglandin E2. Journal of immunology. 2012; 188 (1):21–8. https://doi.org/10.4049/jimmunol.1101029 PMID: 22187483

38. Tanioka T, Nakatani Y, Semmyo N, Murakami M, Kudo I. Molecular identification of cytosolic prostaglandin E2 synthase that is functionally coupled with cyclooxygenase-1 in immediate prostaglandin E2 biosynthesis. The Journal of biological chemistry. 2000; 275(42):32775–82. https://doi.org/10.1074/jbc.M003504200 PMID: 10922363

39. Murakami M, Naraba H, Tanioka T, Semmyo N, Nakatani Y, Kojima F, et al. Regulation of prostaglandin E2 biosynthesis by inducible membrane-associated prostaglandin E2 synthase that acts in concert with cyclooxygenase-2. The Journal of biological chemistry. 2000; 275(42):32783–92. https://doi.org/10.1074/jbc.M003505200 PMID: 10869354

40. Glasauer SM, Neuhauss SC. Whole-genome duplication in teleost fishes and its evolutionary consequences. Molecular genetics and genomics: MGG. 2014; 289(6):1045–60. https://doi.org/10.1007/s00438-014-0889-2 PMID: 25092473

41. Hohl TM, Van Epps HL, Rivera A, Morgan LA, Chen PL, Feldmesser M, et al. Aspergillus fumigatus triggers inflammatory responses by stage-specific beta-glucan display. PLoS pathogens. 2005; 1(3):e30. https://doi.org/10.1371/journal.ppat.0010030 PMID: 16304610

42. Garth JM, Reeder KM, Godwin MS, Mackel JJ, Dunaway CW, Blackburn JP, et al. IL-33 Signaling Regulates Innate IL-17A and IL-22 Production via Suppression of Prostaglandin E(2) during Lung Fungal Infection. Journal of immunology (Baltimore, Md: 1950). 2017; 199(6):2140–8. https://doi.org/10.4049/jimmunol.1602186 PMID: 28784844

43. Garth JM, Mackel JJ, Reeder KM, Blackburn JP, Dunaway CW, Yu Z, et al. Acidic Mammalian Chitinase Negatively Affects Immune Responses during Acute and Chronic Aspergillus fumigatus Exposure. Infection and immunity. 2018; 86(7):e00944–17. https://doi.org/10.1128/IAI.00944-17 PMID: 29712728

44. Lopez-Munoz A, Nicolas FE, Garcia-Moreno D, Perez-Oliva AB, Navarro-Mendoza MI, Hernandez-Onate MA, et al. An Adult Zebrafish Model Reveals that Mucormycosis Induces Apoptosis of Infected Macrophages. Sci Rep. 2018;8(1): 12802–6. https://doi.org/10.1038/s41598-018-30754-6 PMID: 30143654

45. Martínez-Colón GJ, Moore BB. Prostaglandin E(2) as a Regulator of Immunity to Pathogens. Pharmacol Ther. 2018; 185:135–46. https://doi.org/10.1016/j.pharmthera.2017.12.008 PMID: 29274705

46. Medeiros A, Peres-Buzalaf C, Fortino Verdan F, Serezani CH. Prostaglandin E2 and the suppression of phagocyte innate immune responses in different organs. Mediators of inflammation. 2012; 2012:327568. https://doi.org/10.1155/2012/327568 PMID: 23024463

47. Shishikura K, Horiuchi T, Sakata N, Trinh DA, Shirakawa R, Kimura T, et al. Prostaglandin E2 inhibits neutrophil extracellular trap formation through production of cyclic AMP. British journal of pharmacology. 2016; 173(2):319–31. https://doi.org/10.1111/bph.13373 PMID: 26505736

48. Rossi AG O'Flaherty JT. Prostaglandin binding sites in human polymorphonuclear neutrophils. Prostaglandins. 1989; 37(6):641–53. https://doi.org/10.1016/0090-6980(89)90102-0 PMID: 2549574

49. Serezani CH, Chung J, Ballinger MN, Moore BB, Aronoff DM, Peters-Golden M. Prostaglandin E2 suppresses bacterial killing in alveolar macrophages by inhibiting NADPH oxidase. American journal of respiratory cell and molecular biology. 2007; 37(5):562–70. https://doi.org/10.1165/rcmb.2007-0153OC PMID: 17585108

50. Mayer-Barber KD, Andrade BB, Oland SD, Amaral EP, Barber DL, Gonzales J, et al. Host-directed therapy of tuberculosis based on interleukin-1 and type I interferon crosstalk. Nature. 2014; 511(7507):99–103. https://doi.org/10.1038/nature13489 PMID: 24990750

51. Tobin DM, Vary JC Jr., Ray JP, Walsh GS, Dunstan SJ, Bang ND, et al. The lta4h locus modulates susceptibility to mycobacterial infection in zebrafish and humans. Cell. 2010; 140(5):717–30. https://doi.org/10.1016/j.cell.2010.02.013 PMID: 20211140

52. Tobin DM, Roca FJ, Oh SF, McFarland R, Vickery TW, Ray JP, et al. Host genotype-specific therapies can optimize the inflammatory response to mycobacterial infections. Cell. 2012; 148(3):434–46. https://doi.org/10.1016/j.cell.2011.12.023 PMID: 22304914

53. Mendoza SR, Zamith-Miranda D, Takács T, Gacser A, Nosanchuk JD, Guimarães AJ. Complex and Controversial Roles of Eicosanoids in Fungal Pathogenesis. Journal of fungi (Basel, Switzerland). 2021; 7(4):254. https://doi.org/10.3390/jof7040254 PMID: 33800694

54. Erb-Downward JR, Noverr MC. Characterization of prostaglandin E2 production by Candida albicans. Infection and immunity. 2007; 75(7):3498–505. https://doi.org/10.1128/IAI.00232-07 PMID: 17470538

55. Dagenais TR, Chung D, Giles SS, Hull CM, Andes D, Keller NP. Defects in conidiophore development and conidium-macrophage interactions in a dioxygenase mutant of Aspergillus fumigatus. Infection and immunity. 2008; 76(7):3214–20. https://doi.org/10.1128/IAI.00009-08 PMID: 18443090

56. Cayeux SJ, Beverley PC, Schulz R, Dörken B. Elevated plasma prostaglandin E2 levels found in 14 patients undergoing autologous bone marrow or stem cell transplantation. Bone marrow transplantation. 1993; 12(6):603–8. PMID: 7907905

57. Shiau CE, Kaufman Z, Meireles AM, Talbot WS. Differential requirement for irf8 in formation of embryonic and adult macrophages in zebrafish. PloS one. 2015; 10(1):e0117513. https://doi.org/10.1371/journal.pone.0117513 PMID: 25615614

58. Miskolci V, Squirrell J, Rindy J, Vincent W, Sauer JD, Gibson A, et al. Distinct inflammatory and wound healing responses to complex caudal fin injuries of larval zebrafish. eLife. 2019; 8:e45976. https://doi.org/10.7554/eLife.45976 PMID: 31259685

59. Vincent WJ, Freisinger CM, Lam PY, Huttenlocher A, Sauer JD. Macrophages mediate flagellin induced inflammasome activation and host defense in zebrafish. Cellular microbiology. 2016; 18(4):591–604. https://doi.org/10.1111/cmi.12536 PMID: 26468080

60. Walton EM, Cronan MR, Beerman RW, Tobin DM. The Macrophage-Specific Promoter mfap4 Allows Live, Long-Term Analysis of Macrophage Behavior during Mycobacterial Infection in Zebrafish. PloS one. 2015; 10(10):e0138949. https://doi.org/10.1371/journal.pone.0138949 PMID: 26445458

61. Yoo SK, Deng Q, Cavnar PJ, Wu YI, Hahn KM, Huttenlocher A. Differential Regulation of Protrusion and Polarity by PI(3)K during Neutrophil Motility in Live Zebrafish. Developmental cell. 2010; 18(2):226–36. https://doi.org/10.1016/j.devcel.2009.11.015 PMID: 20159593

62. Lim FY, Ames B, Walsh CT, Keller NP. Co-ordination between BrlA regulation and secretion of the oxidoreductase FmqD directs selective accumulation of fumiquinazoline C to conidial tissues in Aspergillus fumigatus. Cellular microbiology. 2014; 16(8):1267–83. https://doi.org/10.1111/cmi.12284 PMID: 24612080

63. Hartmann T, Dümig M, Jaber BM, Szewczyk E, Olbermann P, Morschhäuser J, et al. Validation of a self-excising marker in the human pathogen Aspergillus fumigatus by employing the beta-rec/six site-specific recombination system. Applied and environmental microbiology. 2010; 76(18):6313–7. https://doi.org/10.1128/AEM.00882-10 PMID: 20656854

64. Lim FY, Sanchez JF, Wang CC, Keller NP. Toward awakening cryptic secondary metabolite gene clusters in filamentous fungi. Methods in enzymology. 2012; 517:303–24. https://doi.org/10.1016/B978-0-12-404634-4.00015-2 PMID: 23084945

65. Szewczyk E, Nayak T, Oakley CE, Edgerton H, Xiong Y, Taheri-Talesh N, et al. Fusion PCR and gene targeting in Aspergillus nidulans. Nat Protoc. 2006; 1(6):3111–20. https://doi.org/10.1038/nprot.2006.405 PMID: 17406574

66. Labun K, Montague TG, Krause M, Torres Cleuren YN, Tjeldnes H, Valen E. CHOPCHOP v3: expanding the CRISPR web toolbox beyond genome editing. Nucleic Acids Research. 2019; 47(W1):W171–W4. https://doi.org/10.1093/nar/gkz365 PMID: 31106371

67. Labun K, Montague TG, Gagnon JA, Thyme SB, Valen E. CHOPCHOP v2: a web tool for the next generation of CRISPR genome engineering. Nucleic Acids Research. 2016; 44(W1):W272–W6. https://doi.org/10.1093/nar/gkw398 PMID: 27185894

68. Montague TG, Cruz JM, Gagnon JA, Church GM, Valen E. CHOPCHOP: a CRISPR/Cas9 and TALEN web tool for genome editing. Nucleic Acids Research. 2014; 42(W1):W401–W7. https://doi.org/10.1093/nar/gku410 PMID: 24861617

69. Oliveira E, Casado M, Raldua D, Soares A, Barata C, Pina B. Retinoic acid receptors' expression and function during zebrafish early development. The Journal of steroid biochemistry and molecular biology. 2013; 138:143–51. https://doi.org/10.1016/j.jsbmb.2013.03.011 PMID: 23619336

70. Rosowski EE, Deng Q, Keller NP, Huttenlocher A. Rac2 Functions in Both Neutrophils and Macrophages To Mediate Motility and Host Defense in Larval Zebrafish. Journal of immunology. 2016; 197 (12):4780–90. https://doi.org/10.4049/jimmunol.1600928 PMID: 27837107

71. Huemer K, Squirrell JM, Swader R, LeBert DC, Huttenlocher A, Eliceiri KW. zWEDGI: Wounding and Entrapment Device for Imaging Live Zebrafish Larvae. Zebrafish. 2017; 14(1):42–50. https://doi.org/10.1089/zeb.2016.1323 PMID: 27676647

72. Huemer K, Squirrell JM, Swader R, Pelkey K, LeBert DC, Huttenlocher A, et al. Long-term Live Imaging Device for Improved Experimental Manipulation of Zebrafish Larvae. Journal of Visualized Experiments. 2017(128). https://doi.org/10.3791/56340 PMID: 29155730

73. Schindelin J, Arganda-Carreras I, Frise E, Kaynig V, Longair M, Pietzsch T, et al. Fiji: an open-source platform for biological-image analysis. Nature methods. 2012; 9(7):676–82. https://doi.org/10.1038/nmeth.2019 PMID: 22743772